



Offshore
Wind Evidence
+ Change
Programme

FLOWERS – Floating Offshore Wind Environmental Response to Stressors - WP2 Electromagnetic fields (EMFs)

Author(s): Andrew B. Gill¹, Zoë L. Hutchison², Emma Storey¹, Brian Kneafsey¹, Susana Lincoln¹ and Kirsty Wright³

1- Cefas, 2- Offshore Wind Directorate, Scottish Government, 3- Marine Directorate, Scottish Government

Date: July 2025

Author contributions

Contribution category	Author
Design and funding acquisition	Andrew B Gill, Zoë L Hutchison
Methods development	Andrew B Gill, Brian Kneafsey, Emma Storey
Data and evidence collection	Andrew B Gill, Brian Kneafsey, Emma Storey, Kirsty Wright
Data analysis and visualisation	Andrew B Gill, Emma Storey, Susana Lincoln, Zoë L Hutchison
Writing	Andrew B Gill, Zoë L Hutchison, Brian Kneafsey, Emma Storey, Susana Lincoln, Kirsty Wright

Document Control

Version	Author	Checked	Approved	Date	Description of change
V3	JMR			7/12/2025	Remove references to 4 th Species
V2	JMR			27/11/2025	Minor figure number changes



Contents

1. Background	10
2. EMF measurement and modelling	11
2.1 Information required for a basic magnetic field model (Objective 1)	11
2.2 Basic modelling of existing offshore wind HVAC cables	14
2.3 Field work to collect data on magnetic fields (Objective 2)	15
2.3.1 Materials for measuring EMF	17
2.3.2 Site Accessibility	19
2.3.3 Surveys Transect positioning	19
2.3.4 Power Data from cables	20
2.3.5 Measured Data Handling	21
2.3.6 Data Storage	22
3. EMF Results	22
3.1 Measurements of magnetic fields	22
3.1.1 Region 1 - Norfolk and the Wash	22
3.1.2 Region 2 - Outer Thames	24
3.1.3 Region 3 - Liverpool Bay	25
3.1.4 Region 4 - North Scotland	27
3.1.5 Interconnectors	28
3.1.6 Comparing sensor 1 and 2	29
3.1.7 Biological context of magnetic field measurements	30
3.2 Comparison of measured and modelled magnetic fields	32
3.2.1 Modelled magnetic field using power data	32
3.3 Summary of Objective 2.	34
3.3.1 Floating offshore wind cable considerations	35
4. Species occurrence and distribution (Objective 3)	35
4.1 Focal Species and Species Distribution	35
4.2 Spatial data handling in GIS	36
4.3 Stepwise approach to determining the likelihood of encounter	37
4.3.1 Thornback ray - benthic species	40
4.3.2 European Seabass - Pelagic species	43
4.3.3 Basking shark - migratory species	46
4.3.4 Summary	49
4.3.5 Spatial assessment incorporating depth and temporal occurrence	49
4.3.6 General Considerations for Water Depth and Vertical distribution	49
5. Framework to estimate the likelihood of species encounter (Objective 4)	52
5.1 Stepwise framework to determine the likelihood of EMF encounter for target species – applied to Floating Offshore Wind Developments	54
6. Guidance to apply the framework (objective 5)	58
6.1 Setting the scoping assessment framework in context	59
6.1.1 Step 1. Data compilation	60
6.1.2 Step 2. Two-dimensional Data Presentation	60



6.1.3 Step 3. Two-dimensional Combined Assessment	61
6.1.4 Step 4. Three-dimensional Data Presentation	64
6.1.5 Step 5. Three-dimensional Combined Assessment	65
6.1.6 Step 6. Temporal Data Integration	65
6.1.7 Step 7 Categorise and Report Confidence	66
6.1.8 Step 8. Outcome	66
6.1.9 Moving forward in predicting impacts	67
7. Discussion and Recommendations	68
7.1 Cable magnetic field measurements	68
7.2 Comparing measured and modelled magnetic fields	69
7.2.1 Variability in EMFs	70
7.2.2 A note on electric fields	70
7.3 Receptors	71
7.3.1 Spatial outputs for species occurrence and distribution, and cable routes	71
7.4 The framework	72
7.5 Evidence gaps	72
7.5.1 Subsea power cable EMFs	72
7.5.2 Receptors	73
8. Acknowledgements	75
9. References	76
10. Appendices	78



Figures

Figure 1. Trefoil high voltage AV cable showing the typical materials and their configuration. Diagram from Resner and Paszkiewicz (2021).....	12
Figure 2. The basic relationship between the magnetic field intensity and distance from the cable axis.	13
Figure 3. Log-log plot of the expected relationship between magnetic field intensity and perpendicular distance. The blue symbols show the relationship $1/r^2$, where r is the distance from the cable centre.....	13
Figure 4. Magnetic field profiles across the surface of the seabed for 10 HVAC subsea cables. The colours of the plots represent the names of the cables shown in the legend (from Normandeau et al. 2011).	14
Figure 5. Typical plot of the magnetic field intensity and propagation with distance from the cable axis for three types of subsea power cable installed at UK offshore wind farm sites.....	15
Figure 6. Log-log relationship for 33 kV, 132 kV and 220 kV cables based on existing UK offshore wind farm operational sites.	15
Figure 7. Map of four areas where existing offshore wind HVAC export cables come to shore and the routes of HVDC interconnectors: 1) North Norfolk and The Wash; 2) Outer Thames; 3) Liverpool Bay; 4) North Scotland. From Global Offshore Renewables Map 4C Offshore.	16
Figure 8(a) Magnetometer set up used for field surveys. Black magnetometers were set up in the same horizontal orientation but were separated 0.5 m vertically. Yellow 20 m cables from the magnetometers were attached to (b) The Spectramag-6 Data Acquisition Unit which was linked to a laptop with the Spectramag-6 software.	17
Figure 9. Spectramag-6 software outputs. Screenshot of the magnetometer outputs showing typical data collected at a site, (a) Example of the range of magnetic field intensities for x, y and z planes and total recording during a 30-second sample period of an AC cable. (b) Example of the magnetic field intensities in relation to the magnetic field frequency.....	18
Figure 10. (a) Example of surveying in the water parallel to the transect sample points marked by red and green coloured flags. (b) Example of a magnetometer measurement frame on a dried mudflat, which was inaccessible at high tide.	19
Figure 11. Depiction of survey transect layout. The red arrowed, broken lines show the path of the survey perpendicular to the cable axis (yellow lines). Yellow stars indicate the survey points at 100, 75, 50, 25, 20, 15 and 10 m. The green rounded rectangle shows zone 10 m on either side of the estimated cable axis. The expanded green rectangle shows 1 m survey points at 1m intervals). Source: Base map is from Google Maps.	20
Figure 12. Measurements at export cable sites showing on the left magnetic field intensity for Sensor 1 (orange) and Sensor 2 (green) in relation to distance from the cable (at 0 m). Site (a) had 33kV cables and there were two site visits, one in July (a1) and the second in September (a2). Site (b) had 132kV cables and site (c) 220kV cables, within Region 1.	23



Figure 13. Measurements at two 132 kV sites and a 150 kV site within Region 2 shown on the left, with magnetic field intensity for Sensor 1 (orange) and Sensor 2 (green) in relation to distance from the cable (at 0 m). Note: at sites (b) and (c) Sensor 2 was not working properly; therefore, data were removed.....	25
Figure 14. Measurements at three 132 kV sites and a 220 kV site within Region 3. (a) 1 x 132 kV HVAC cables, (b) 1 x 132 kV HVAC cables, (c) 2 x 220 kV HVAC, and (c) 4 x 132 kV HVAC cables. Magnetic field intensity for Sensor 1 (orange) and Sensor 2 (green) in relation to distance from the cable (at 0 m).....	27
Figure 15. Measurements at two 132 kV export cable sites within Region 4 are shown on the left, with magnetic field intensity for Sensor 1 (orange) and Sensor 2 (green) in relation to distance from the cable (at 0 m).....	28
Figure 16. Field measurements for two interconnector sites within (a) Region 2 and (b) Region 4, showing the overall magnetic field intensity maximum (blue and white circles) and minimum recordings (black circles) in relation to distance from the cable (at 0 m). The red broken line shows the background geomagnetic field intensity for the location, based on the International Geomagnetic Reference Field (IGRF) Calculator via the British Geological Society.....	29
Figure 17. Relationship between Sensor 1 and Sensor 2, standardised for the current generating the measured magnetic field.....	30
Figure 18. Relationship between the magnetic field measured and distance from cable, standardised per unit electrical current, for five cable surveys (2 x 33 kV, 2 x 132 kV and 1 x 220 kV). Enlarged grey points highlight coincident black and grey data values.	30
Figure 19. The ability of marine organisms to detect magnetic fields is represented on the left, based on their known range of detectability, for the purposes of comparison to the measured and modelled magnetic fields from HVAC cables, on the right. The range of magnetic field intensities is from nanotesla to milliTesla. Magnetic fields are presented with distance from each cable (up to 25m) measured at multiple export cable sites and overlaid with models of three typical HVAC export cables (33kV, 132kV and 220k) at maximum power. The magnetic field intensities measured were within the microTesla range, which overlaps with the known range of detectability by marine organisms.....	31
Figure 20. Log-log comparison of measured and modelled data at four different sites. (a) and (b) Norfolk and The Wash (33 kV), (c) Outer Thames (132 kV), (d) Liverpool Bay (132 kV), and (e) Liverpool Bay (220kV). Dotted lines show best fitting curve with equation of the line and the coefficient of determination (R^2). ...	34
Figure 21. Overlay of thornback ray habitat suitability and fixed offshore wind farm EMFs zone footprints (including the export cable route) in Region 2. The darker the blue square, the more suitable the habitat associated with the species. The pink areas represent the offshore wind installation footprint with the 50 m EMF zone relating to the extent of the magnetic field in the marine environment for the whole offshore wind infrastructure development.	41
Figure 22. Overlay of European seabass habitat suitability and fixed offshore wind farm footprints (including the export cable route) in Region 1 and part of Region 2. Owing to the coarser scale of the seabass habitat suitability data, the scale was widened to include two adjacent regions where seabass occurred. The darker the blue square, the more suitable the habitat was for the species. The pink areas represent the offshore	

wind installation footprint with the 50 m EMF zone relating to the extent of the magnetic field in the marine environment associated with the offshore wind infrastructure.....	44
Figure 23. Overlay of Basking shark habitat suitability and fixed offshore wind farm footprints (including the export cable route) in Region 3. The darker the blue data square the more suitable the habitat was for the species. The pink areas represent the offshore wind installation footprint with the 50 m EMF zone relating to the extent of the magnetic field in the marine environment associated with the offshore wind infrastructure.....	47
Figure 24. Depiction of the relationship between target species depth ranges (dotted arrows) and the location of the subsea power cable EMF zones for buried cables from fixed offshore wind (left) and dynamic cables from floating offshore wind (right). The vertical position and habitat range in the water column of different receptors and life stages will determine how likely they will encounter the EMFs generated by the power cable. Image credits: pelagic, juvenile fish and benthic invertebrate icons from Vecteezy, benthic fish icon from Noun Project.	52
Figure 25. The essential elements identified through the FLOWERS project to determine the likelihood of encounter between focal species and subsea power cable EMFs. These elements are demonstrated in prior sections of the report through Objectives 1, 2, and 3.....	53
Figure 26. The stepwise framework for determining the likelihood of encounter between a focal receptor and EMFs associated with subsea power cable areas. The eight step framework should be used for each species and life history stage of interest. The framework presents an iterative approach to data compilation and presentation (including assignment of data confidence), a combined spatial assessment in 2D and subsequently 3D, with consideration of temporal occurrence of the receptor taxa. The return loop ensures that, where further spatial or ecological data are required, they can be sourced and integrated before a suitable assessment of the likelihood of encounter can be made. This framework is an effective scoping assessment of EMF enabling a justified decision to scope into or out of the Environmental Impact Assessment process.....	56
Figure 27. The two-dimensional data presentation for basking sharks and EMF zones associated with floating offshore wind in the Celtic Sea. The eastern Celtic Sea habitat suitability for basking sharks is presented from multiple data sources with a medium data confidence. The Round 5 offshore wind planning area is included, represented with the pink-coloured EMF zone applied. Note: The planning area assumes that floating offshore wind will occur across the extent shown. However, the export cable routes are not included due to unavailability at the time of the scoping assessment.	62
Figure 28. The evidence needs for an effective approach to predicting EMF impacts on focal receptors in the aquatic environment. The likelihood of encounter assessment can be considered a precursor to build upon in establishing an encounter rate for a species that is likely to encounter an EMF.	68

Tables

Table 1. The UK coastal regions and cable types visited to measure magnetic field fields from in situ operational subsea power cables.....	16
Table 2. List of the focal species and their attributes, selected for spatial occurrence and distribution analysis within EMF fieldwork regions.	36
Table 3. Weighting to apply to GIS species data grid square categories (the example here relates to habitat suitability). Note: The number of rows can be adjusted according to the GIS categorisation chosen, to ensure the best representation of the data.....	38
Table 4. A table template for compiling data to determine the likelihood of 2D spatial overlap (per development and/or defined region). The blue cells in the table are the weighted proportions on which to apply criteria for the 2D likelihood of encountering the EMF zones for the defined region (column E) or each offshore wind development (columns Gi, Gii, Giii, etc). The green cell represents the spatial confidence of the data for the region based on the green table categories.	39
Table 5. Likelihood of encounter for the benthic thornback ray determined from 2D spatial overlap assessment of species occurrence and EMFs zones. Categories are: a) <25% = low; b) 25-50% = low-medium; c) 50-75% = medium-high; or d) >75% = high. Confidence level is based on the proportion of spatial grid squares with data in relation to the total number of grid squares in the region (i.e. no data; see Likelihood of spatial overlap data Table 4).	42
Table 6. The 2D likelihood of encounter for European seabass determined from spatial overlap assessment of species occurrence and EMFs zones. Categories are: a) <25% = low; b) 25-50% = low-medium; c) 50-75% = medium-high; or d) >75% = high. Confidence level is based on the proportion of spatial grid squares with data in relation to the total number of grid squares in the region (i.e. no data; see Likelihood of spatial overlap data table).	45
Table 7. The 2D likelihood of encounter for basking shark determined from spatial overlap assessment of species occurrence and EMFs zones. Categories are: a) <25% = low; b) 25-50% = low-medium; c) 50-75% = medium-high; or d) >75% = high. Confidence level is based on the proportion of spatial grid squares with data in relation to the total number of grid squares in the region (i.e. no data; see Likelihood of spatial overlap data table).	48
Table 8. Summary of vertical and temporal distribution ranges for the three focal species used to estimate spatial overlap with SPC EMFs. The depth ranges represent the most frequent depths that the species inhabit, based on the sources cited. Temporal aspects included represent the seasons in UK waters: Spring (Mar – May); Summer (Jun - Aug); Autumn (Sep – Nov); Winter (Dec - Feb).	50
Table 9. The confidence categories and the associated criteria for the 2D, 3D and temporal data separated into EMF and Receptor criteria.	58
Table 10. The focal receptor and their attributes, selected for spatial occurrence and distribution analysis within EMF fieldwork region of interest. This information is repeated from Table 2, for ease of the reader.	60

Table 11. Likelihood of encounter for basking shark determined from 2D spatial overlap assessment of species occurrence and EMFs zones of floating offshore wind developments in the Celtic Sea.....	63
Table 12. Summary of vertical distribution ranges for the basking shark. The depth ranges represent the most frequent depths inhabited, based on literature sources cited. Variation in vertical distribution are included, for UK waters: Spring (Mar – May); Summer (Jun - Aug); Autumn (Sep – Nov); Winter (Dec - Feb). This information is repeated from Table, for ease of the reader.....	65
Table 13. Summary of the likelihood of encounter for basking sharks, determined from spatial overlap assessment of habitat suitability and EMFs zones associated with floating offshore wind developments. The likelihood of encounter for the region and individual developments is summarised in (a) and the confidence metrics for each data set with the spatial confidence for the region is detailed in (b). Likelihood of encounter categories are: a) <25% = low; b) 25-50% = low-medium; c) 50-75% = medium-high; or d) >75% = high. Spatial confidence level is based on the proportion of spatial grid squares with data in relation to the total number of grid squares in the region (i.e. no data; see Likelihood of spatial overlap data table). For assessment data see Table, in Step 3	66

The FLOWERS project forms part of the Offshore Wind Evidence and Change programme, led by The Crown Estate in partnership with the Department for Energy Security and Net Zero and Department for Environment, Food & Rural Affairs. The Offshore Wind Evidence and Change programme is an ambitious strategic research and data-led programme. Its aim is to facilitate the sustainable and coordinated expansion of offshore wind to help meet the UK's commitments to low carbon energy transition whilst supporting clean, healthy, productive and biologically diverse seas.

1. Background

Electromagnetic Fields (EMFs) exist naturally and through human activities across the global environment, and interest in how animals might use or be affected by EMFs is growing. There are two primary EMF components: a magnetic field and an electric field. These components interact with each other and can induce one another. Natural magnetic fields are found throughout the environment, they include the Earth's geomagnetic field and natural electric fields are represented by the bioelectric fields directly created by all living animals, and the motional electric fields induced by water movement through the geomagnetic field. Owing to the ubiquity of EMFs in the environment, all organisms experience natural EMFs. Many species are known to be able to respond with behavioural, physiological, biochemical or genetic outcomes when exposed to EMFs, yet only some have known specific receptors for magnetic field or electric field detection (Albert et al., 2020; Gill and Desender 2020; Hutchison and Gill, 2025; Nyqvist et al., 2020).

Anthropogenic EMFs are associated with any device or technology that uses electricity and/or magnetic materials. Of particular interest to the FLOWERS project is the transmission of electricity through subsea power cables (SPCs), including dynamic cabling used within floating offshore renewable projects. The electric current flowing through the SPCs creates direct magnetic fields outside the cable into the adjacent environment. This, in turn, can induce electric fields. Therefore, to understand the nature and extent of anthropogenic EMFs, it is helpful to focus on the directly emitted magnetic field as the primary emission experienced by organisms. This is true of whether the power cable is buried, or surface laid and covered in cable protection (as seen with fixed offshore wind), or SPCs in the water column (i.e. dynamic cables) associated with floating offshore wind (FLOW). The magnetic field created is not affected by the material around it unless it has magnetic properties. The magnetic field emitted from the cable will then determine the intensity, frequency and extent of the electric field that is induced in the adjacent environment.

The spatial extent and intensity of the EMFs associated with a cable, primarily depend on the materials and their electrical properties as well as the power being transmitted; together referred to here as the cable characteristics. These cable characteristics and the resulting EMFs need to be specified so that they can be assessed in terms of whether there is any impact on organisms of interest. Before the consideration of environmental impact, it is important to determine if the receptor species encounter the EMFs associated with SPCs within the 3-dimensional aquatic environment. Determining the likelihood of encounter between focal species and SPC EMFs was the central aim of the FLOWERS WP2.

FLOWERS WP2 builds on findings and outputs from a series of research projects and EMF expert consultations that the project partners have been leading over recent years. These efforts have focused on determining how best to define and assess the EMF environment associated with subsea power cables that could be encountered by organisms of interest. To date, our primary focus has been on fixed offshore wind farm (OSW) High Voltage Alternating Current (HVAC) cables and High Voltage Direct Current (HVDC) cables, including interconnector cables. FLOWERS WP2 was directed at floating offshore wind developments, and their dynamic cables with regard to EMFs. As the magnetic fields created by the transmission of electricity is similar whether cables are buried, on the seabed, in the water column or in the air, we were able to apply existing knowledge from fixed OSW to the FLOW case (*note*: the situation with electric fields is much more complex as they are determined

both by the characteristics of the environment and the cables, therefore they were not the focus of the FLOWERS project).

WP2 of FLOWERS aimed to address the knowledge gaps on EMFs associated with dynamic cables through meeting the following objectives:

- *Objective (1) Define the key attributes of the magnetic field component of the EMF associated with subsea cables (both on the seabed and in the water column) through building on simple EMF emission models (for application to floating offshore wind).*
- *Objective (2) Verification of magnetic field component of the EMF model related parameters through in situ data collection.*
- *Objective (3) Estimation of the temporal and spatial overlap between selected EM-sensitive species and cabling routes.*
- *Objective (4) Development of a first version approach to estimate the likelihood of species encounter as a proxy to inform the potential risk of EMF exposure to target species.*
- *Objective (5) A set of guidance based on the methods to determine the magnetic field component of the EMF and the likelihood of encounter using the outputs from the other objectives.*

The outputs are anticipated to be useful in that they provide an effective scoping assessment of EMFs as an environmental stressor and, therefore, determining whether EMFs should be included in the subsequent environmental impact assessment process. If there is the likelihood of encountering EMFs, then the outputs will assist in the EIA process and can be built upon. Incorporating the likelihood of encounter will reduce the uncertainty and increase confidence associated with assessing the potential risk to EM-receptive taxa and taxa that may be exposed but where their receptive abilities are not known. The approach set out in WP2 uses fixed OSW to develop and exemplify the approach, which is then provided as a step-by-step framework. The application of the framework is then illustrated in guidance through a case study applicable to FLOW.

2. EMF measurement and modelling

2.1 Information required for a basic magnetic field model (Objective 1)

Magnetic fields created by the flow of electrical current within any cable can be approximated for a two-dimensional (2D) cable cross-section using widely available equations (EPRI, 2022). The correct equation will depend on the number of conducting wires (known as cores or phases) and their cross-sectional relationship within a cable. There are more sophisticated modelling tools available; however, these tend to be proprietary software, requiring many more details to parameterise the models and the appropriate engineering expertise to use the tools and interpret the outputs. The purpose of the basic modelling undertaken in the FLOWERS WP2 objective 1, was to apply a freely available method that is relatively easy to use and interpret and often used during environmental assessment of EMFs associated with subsea power cables. The discussion (Section 4)

highlights further parameters that should be considered to increase the realism of a model's approximation of the EMFs, including those associated with dynamic cables.

The most common cable type and configuration used today for offshore wind electricity transmission (whether fixed or floating) is bundled, trefoil 3-core HVAC cables (note: High Voltage Direct Current, HVDC cables are expected to be included in the cabling used for floating offshore wind in the future as developments occur farther offshore (Bresesti et al, 2007;), however HVAC cabling is expected to be used within the floating turbine array). Here we focus on HVAC as it allowed measurements to be taken of subsea power cables and therefore comparison with modelling. For HVAC, there are three identical conducting wires equidistant from each other, bundled within an overall protection and armoured casing (Figure 1).

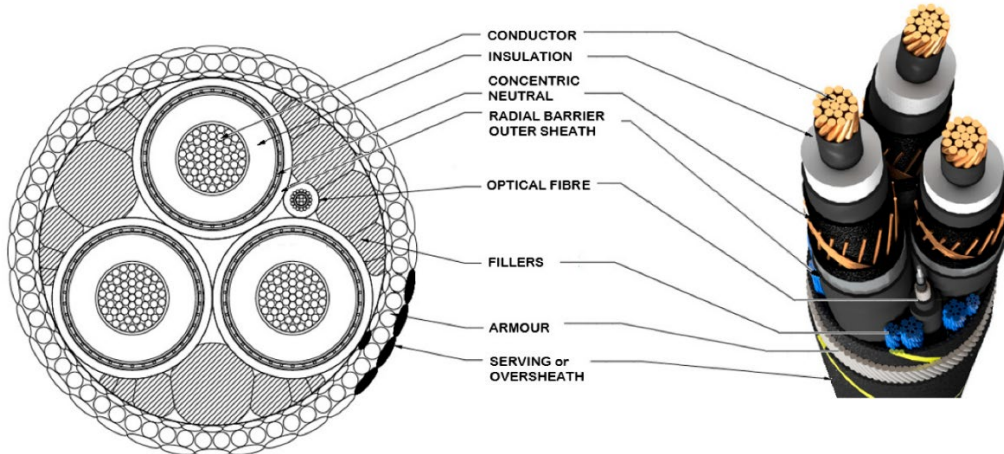


Figure 1. Trefoil high voltage AV cable showing the typical materials and their configuration. Diagram from Resner and Paszkiewicz (2021).

Parameters were identified based on the rationale set out and agreed by a group of experts during an OWEC funded EMF workshop (Gill et al., 2023; Appendix 1). At the EMF workshop, the minimum parameters required for basic modelling of the magnetic field used within existing permitting/licensing considerations were split into the cable EMF (i.e. the energy emission only) and the cable within the environment. Following this approach, the parameters were specified as (see Approach (a) and (b) in Appendix 1 for further details):

- electric current
- relative coordinates of the centre of the cable and the centre of the cores
- distance in the adjacent environment from the centre of the cable

These parameters were used to calculate the intensity of the resultant magnetic field (B field, microTesla; μT) using the following equation (EPRI, 2022):

$$B \text{ field} = \frac{\sqrt{2} \cdot 3R_o I}{r^2} \div 10 \mu\text{T} \quad (\text{i})$$

where R_o = radius of the centre of a conductor to the centre of the whole cable (cm; see Figure 1), I = current (Amps) and r = distance from the centre of the cable to a point in the environment, perpendicular to the cable axis.

The equation assumes that the three cable cores form an equilateral triangle, which is the standard configuration of offshore wind HVAC export cables: that the cores are parallel and lying in a straight line as they appear in Figure 1. A further assumption is that the electrical current in each of the conducting cores is balanced; taken together, this is termed the phase current.

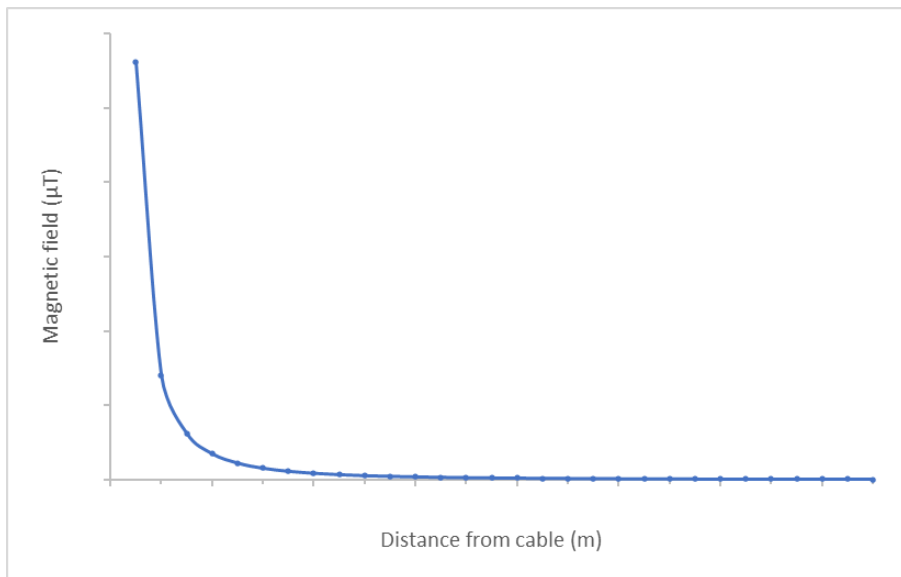


Figure 2. The basic relationship between the magnetic field intensity and distance from the cable axis.

The calculation of the magnetic field intensity with distance results in a two-dimensional curve that describes the propagation of the magnetic field intensity with perpendicular distance from the cable (Figure 2).

Owing to the symmetrical and curvilinear relationship obtained from such modelling, the magnetic field intensity and distance from the cable are often described using log-log plots (Figure 3). The propagation of the B-field associated with a balanced phase-current is predicted as $1/r^2$ where r is the distance from the cable centre (Figure 3).

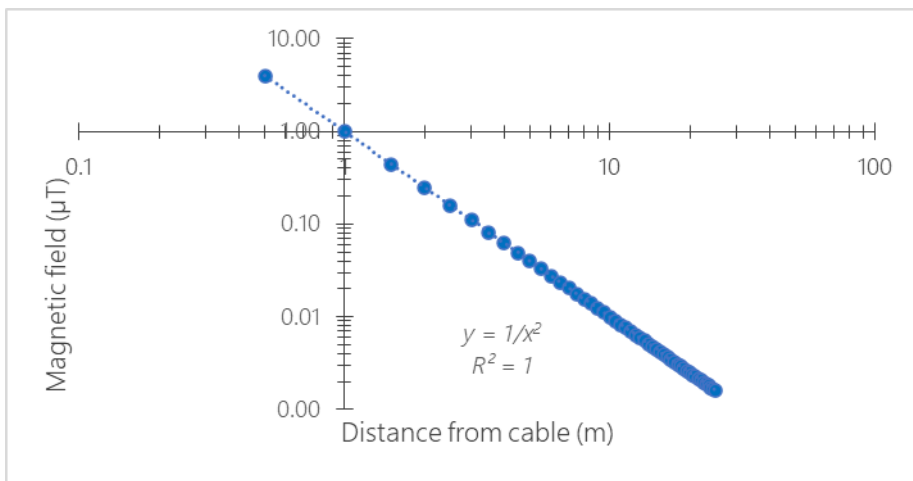


Figure 3. Log-log plot of the expected relationship between magnetic field intensity and perpendicular distance. The blue symbols show the relationship $1/r^2$, where r is the distance from the cable centre.

To date, the modelling of EMF associated with subsea cables has used models to estimate the maximum magnetic field intensity at the surface of the seabed with increasing distance from the cable axis location. Figure 4 shows plots for several existing SPCs based on modelling the magnetic field (μT) at the surface of the seabed for cables buried between 0.5 and 2 m (from Normandeau et al. 2011). Such plots are commonly used to describe the magnetic field environment that receptors organisms will encounter. In these plots, the maximum magnetic field intensity is over the cable axis (i.e. 0 m along the seabed surface) and there is a curvilinear decline in intensity with distance, which reflects the general relationship shown in Figure 2 and Figure 3, but on both

sides of the cable. In the context of floating offshore wind SPC, the modelling will need to include the magnetic and induced electric fields from the cable surface. Which may therefore require a revised modelling approach and depiction of the magnetic field at the surface and its propagation with distance from the cable.

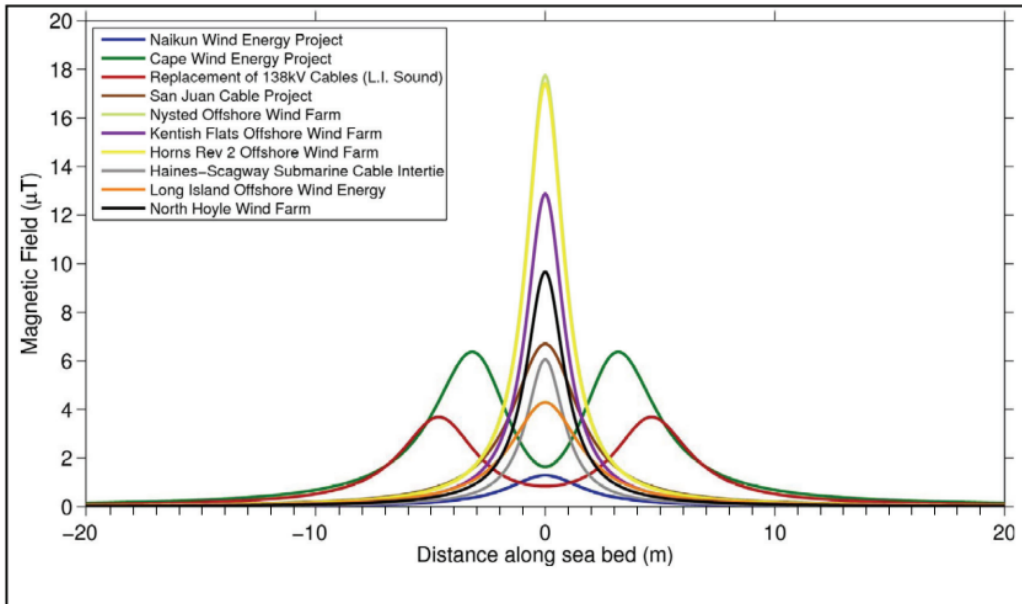


Figure 4. Magnetic field profiles across the surface of the seabed for 10 HVAC subsea cables. The colours of the plots represent the names of the cables shown in the legend (from Normandeau et al. 2011).

2.2 Basic modelling of existing offshore wind HVAC cables

To obtain realistic predictions of the magnetic field of industry standard 33 kilovolts (kV), 132 kV and 220 kV alternating current (AC) subsea power cables, we requested details of the materials and characteristics from the cable transmission operators for several sites around the UK (see Figure 6 and Table 1). From the details received, the magnetic field modelling approximation was undertaken using equation (i) for different 0.5 m distances from the cable (Figure 4).

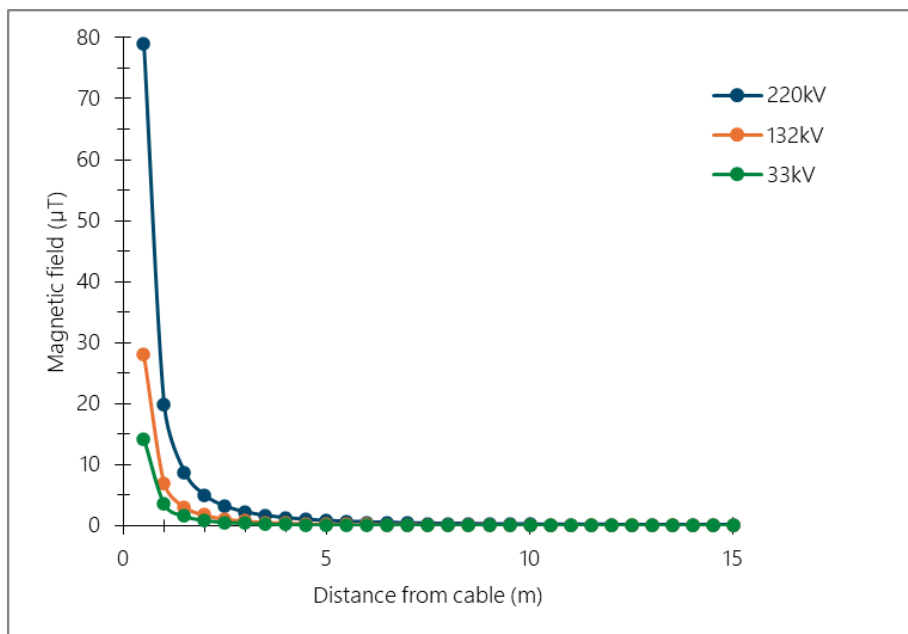


Figure 5. Typical plot of the magnetic field intensity and propagation with distance from the cable axis for three types of subsea power cable installed at UK offshore wind farm sites.

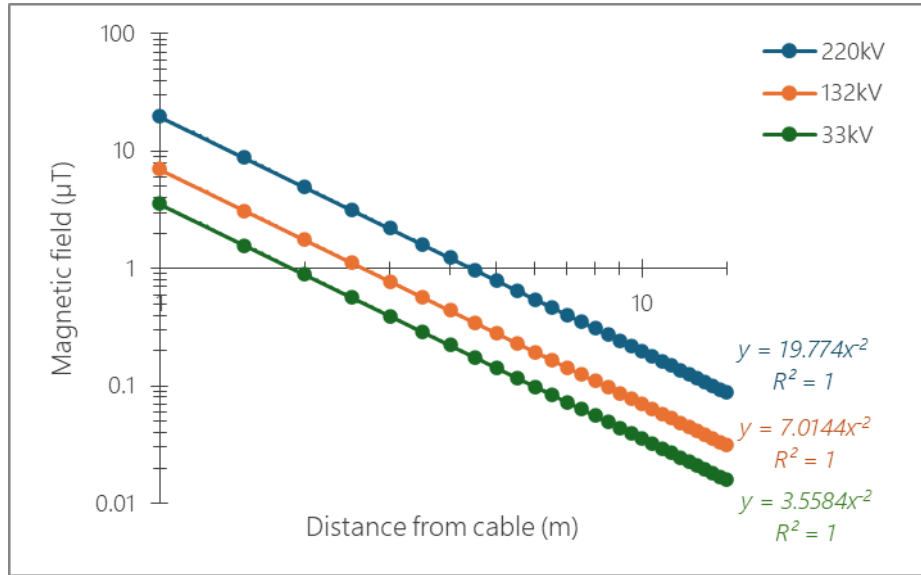


Figure 6. Log-log relationship for 33 kV, 132 kV and 220 kV cables based on existing UK offshore wind farm operational sites.

The modelling predicted that the highest intensity of the magnetic field will be above the cable axis, and the intensity will decrease rapidly with distance (Figure 5). The larger the voltage-rated cable is, the larger the predicted intensity of the magnetic field created. This is particularly evident within 5 m on either side of the cable compared to the lower voltage-rated cables. The combination of the lower electrical current transmitted by the cable and the configuration of the cable cores causes this difference. Whilst the relationships appear to converge the further away from the cable (Figure 5). The log-log plot shows the model maintains the relative difference according to the $1/r^2$ relationship (Figure 6).

2.3 Field work to collect data on magnetic fields (Objective 2)

Existing, freely available data on EMFs associated with subsea power cables are very sparse; however, it is relatively straightforward to measure the local magnetic fields (but not electric fields) of existing cables. Whilst the FLOWERS project set out to address environmental pressures associated with floating offshore wind, there are limited sites available with dynamic cables globally and accessing the cables is currently extremely challenging.

Magnetic fields are a component of the EMFs and the primary emission from electricity transmission, independent of whether the cable is buried, in open water or the air. Therefore, to meet objective 2 and provide a comparison between the model approximation and the subsea power cable magnetic fields created in the environment, we chose to measure the magnetic field of export cables from operational fixed offshore wind sites.

During June and July to October 2024, we visited 12 sites within four geographic areas around the UK coast (Figure 7; Table 1). Within these areas field measurements of the export cables were undertaken across a distance gradient perpendicular to the cable route at landfall. These measurements were then compared with

the model estimations (magnetic component determined in Objective 1). A selection of operational offshore wind export HVAC cables were measured, as well as two HVDC interconnectors (Table 1).

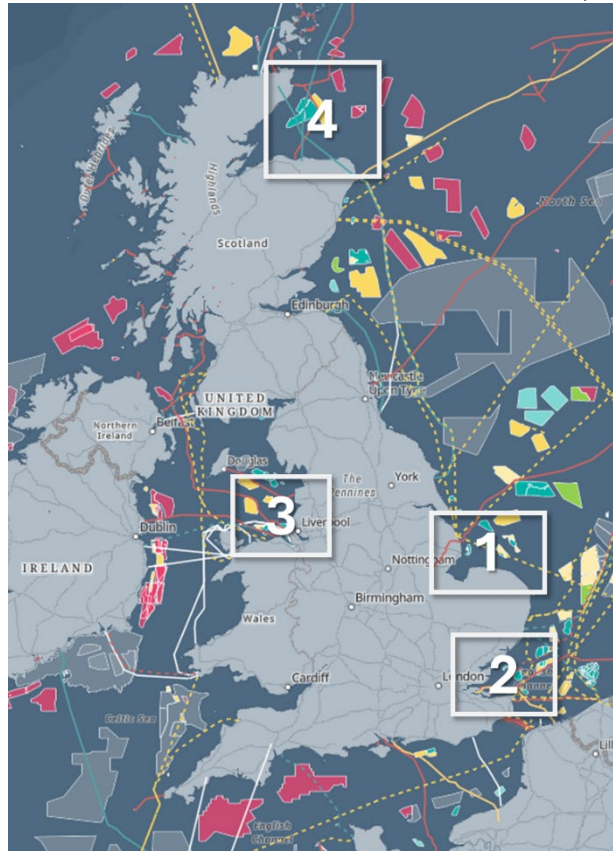


Figure 7. Map of four areas where existing offshore wind HVAC export cables come to shore and the routes of HVDC interconnectors: 1) North Norfolk and The Wash; 2) Outer Thames; 3) Liverpool Bay; 4) North Scotland. From [Global Offshore Renewables Map | 4C Offshore](#).

Table 1. The UK coastal regions and cable types visited to measure magnetic field fields from in situ operational subsea power cables.

Region	Cable type (OSW Export / Interconnector)	Cable transmission (AC/DC)	Cable Type (kV)
1. Norfolk and The Wash	OSW Export	HVAC	132
1. Norfolk and The Wash	OSW Export	HVAC	33
1. Norfolk and The Wash	OSW Export	HVAC	220
2. Outer Thames	OSW Export	HVAC	132
2. Outer Thames	OSW Export	HVAC	150
2. Outer Thames	OSW Export	HVAC	132
2. Outer Thames	Interconnector	HVDC	400
3. Liverpool Bay	OSW Export	HVAC	132
3. Liverpool Bay	OSW Export	HVAC	132

Region	Cable type (OSW Export / Interconnector)	Cable transmission (AC/DC)	Cable Type (kV)
3. Liverpool Bay	OSW Export	HVAC	220
3. Liverpool Bay	OSW Export	HVAC	132
4. North Scotland	OSW Export	HVAC	220
4. North Scotland	OSW Export	HVAC	220
4. North Scotland	Interconnector	HVDC	320

2.3.1 Materials for measuring EMF

Two Bartington (3 axis mag-13, +/- 1000 µT) magnetometers were mounted in the same orientation on a sturdy plastic frame (with nylon screws; Figure 8a). The lower magnetometer was attached at the base of the frame and the second 0.5 m vertically above (Figure 8a). Each magnetometer had a separate cable (20 m length) attached with the other end connected to the Bartington Spectramag-6 data acquisition unit (Figure 8b). The unit logged the data, which was displayed on a linked laptop with the Spectramag-6 software to display and record the data collected (Figure 9).



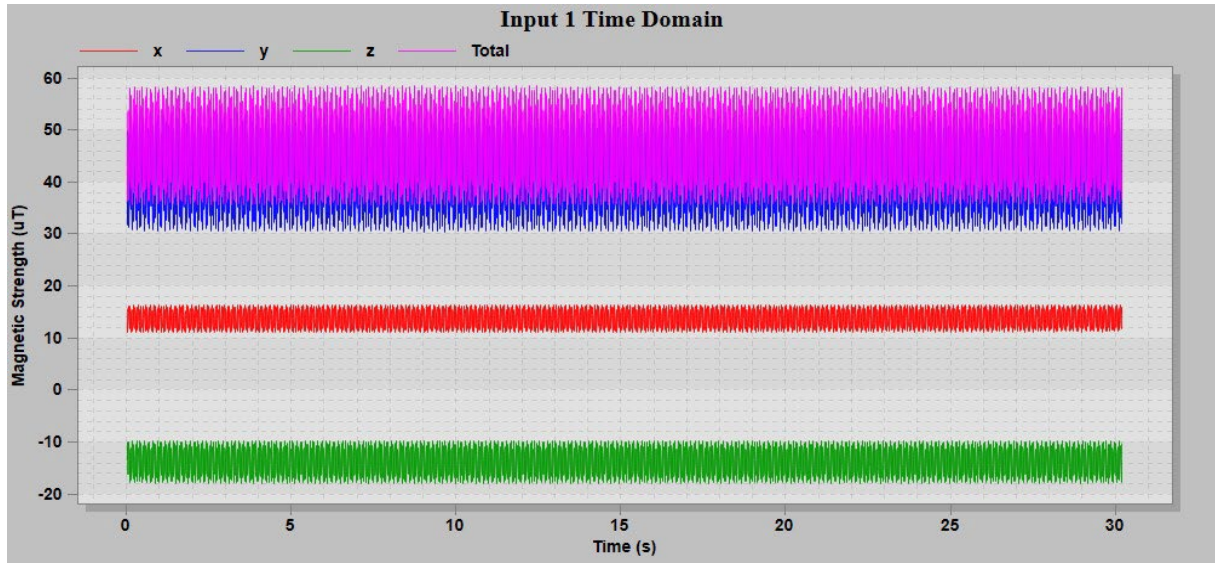
(a)



(b)

Figure 8(a) Magnetometer set up used for field surveys. Black magnetometers were set up in the same horizontal orientation but were separated 0.5 m vertically. Yellow 20 m cables from the magnetometers were attached to (b) The Spectramag-6 Data Acquisition Unit which was linked to a laptop with the Spectramag-6 software.

(a)



(b)

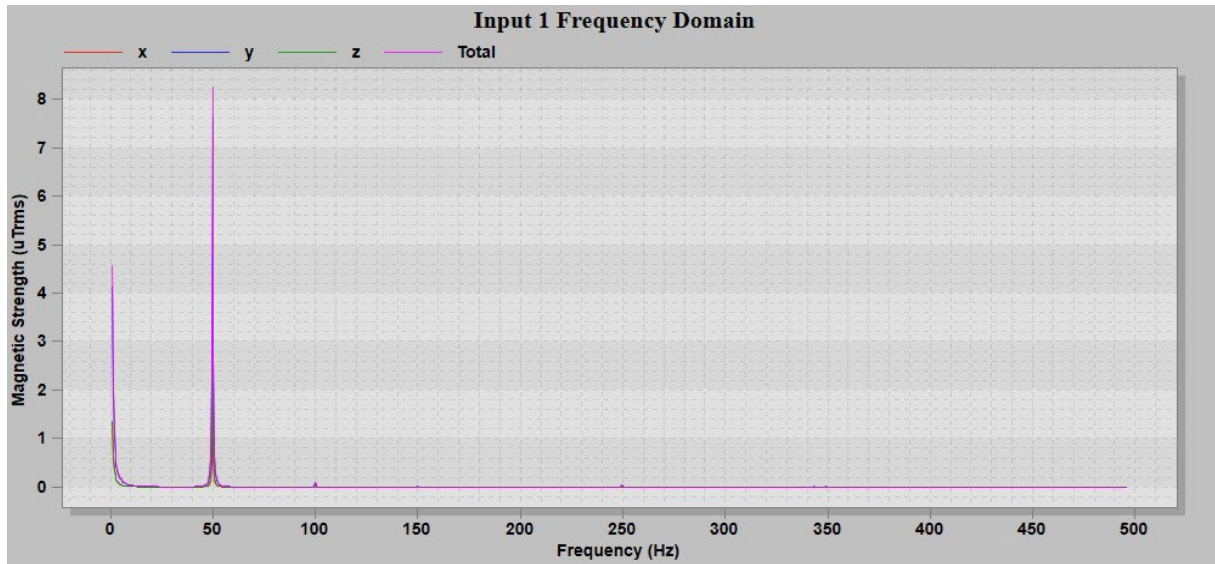


Figure 9. Spectramag-6 software outputs. Screenshot of the magnetometer outputs showing typical data collected at a site, (a) Example of the range of magnetic field intensities for x, y and z planes and total recording during a 30-second sample period of an AC cable. (b) Example of the magnetic field intensities in relation to the magnetic field frequency.

Each EMF sensor had three axes, independently measuring the magnetic field in the x, y and z planes. The sensors measured the frequency and the intensity of the magnetic fields. Therefore, the natural magnetic fields at a location (e.g. Earth's geomagnetic field) were recorded in addition to the 50 Hz AC magnetic field or DC magnetic field produced by the power cables.

The Spectramag outputs shown in Figure 9 (a and b), display the data for each of the 3 axes (x, y, z) individually and the total combined magnetic field. Figure 9b shows the DC background geomagnetic field around 0 Hz and the AC peak around 50 Hz. The smaller peaks at 100 Hz and 250 Hz represent harmonics of the 50 Hz signal. For

the DC interconnector cables, the frequency and intensity reflected the interaction between the DC geomagnetic field and the cable (not shown).

2.3.2 Site Accessibility

The locations visited were chosen based on discussions with cable operators (either the offshore transmission operators, OFTOs; or the offshore wind farm operator of the site), with the aim of collecting measurements across the UK in different regions where several HVAC offshore wind export cables were located. In two areas, we took advantage of the proximity of HVDC interconnectors (Table 1). Each site was assessed for accessibility in the intertidal zone and survey logistics to ensure HSE compliance for safe and effective data collection. Power cable routes and sites details were obtained from the cable operating company and through reviewing freely available spatial data on the 4COffshore ([Global Offshore Renewables Map | 4C Offshore](#)) and KIS-ORCA ([Map | KIS-ORCA](#)) websites, which were used to determine the GPS coordinates of the buried cables.

In most cases we had 'as-built' cable route information provided by the OFTOs and at some sites there were markers indicating the approximate location of separate cables. Overall, it was challenging to identify the buried cable route accurately, and in some cases the cables were horizontally directionally drilled (HDD) deep below the intertidal zone. To assist with identifying the buried cable route, we used a handheld EMF meter for AC cables to determine where the intensity was highest at the seabed/beach/intertidal zone surface. The orientation of the cable was estimated using a compass bearing estimated from the spatial data sources. We also had to ensure that we did not go too far up-shore as 3-core subsea power cables are often split into single core before reaching the onshore substation. Cable plans were consulted where available to ensure we were in approximately the right place.

2.3.3 Surveys Transect positioning

When on site, a dynamic risk assessment was conducted to determine the safe positioning of the survey transect. Surveys were undertaken in the intertidal zone, in <1 m of water, where it was safe to do so (Figure 10a). Otherwise, surveys were conducted at the nearest safe and accessible point on land to the subsea cable landfall locations (e.g. Figure 10b).



Figure 10. (a) Example of surveying in the water parallel to the transect sample points marked by red and green coloured flags. (b) Example of a magnetometer measurement frame on a dried mudflat, which was inaccessible at high tide.

At each site, a 100 m transect was laid out with flag markers perpendicular to the cable axis (Figure 10). The cable axis was determined from spatial data obtained through the online sources or following 'as-laid' cable route GPS coordinates where available. The magnetometer frame was positioned at points 100, 75, 50, 25, 20, 15 and 10 m, and then every metre from 10 to -10 m from the cable. The 1 m interval data points crossed the estimated cable axis; however, as the cable was not visible, data points on either side ensured that we captured the highest intensity readings in proximity to the cable axis. At each point, the EMF intensity and frequency were recorded for 30 seconds.

Most sites had more than one export cable coming ashore. We therefore set out the transects as per Figure 10, based on one of the outside cables. Once past the cable axis +/- 10 m zone, we measured every 2 m over an extended transect up to and including the estimated location of the last cable.

GPS coordinates were recorded at each of the starred data collection points (Figure 10) and the estimated location of each export cable, if there was more than one cable. These GPS data were later used to represent the transects and the measurement positions on a map of the area.

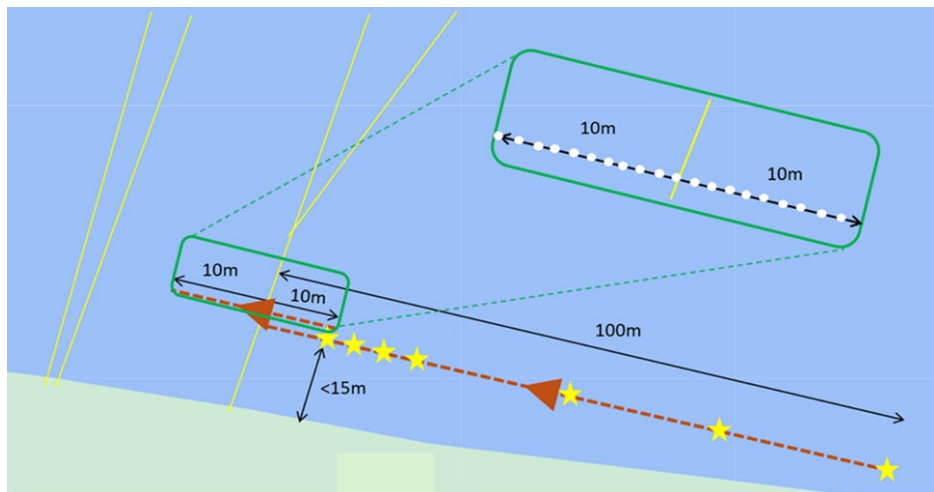


Figure 11. Depiction of survey transect layout. The red arrowed, broken lines show the path of the survey perpendicular to the cable axis (yellow lines). Yellow stars indicate the survey points at 100, 75, 50, 25, 20, 15 and 10 m. The green rounded rectangle shows zone 10 m on either side of the estimated cable axis. The expanded green rectangle shows 1 m survey points at 1m intervals).

Source: Base map is from Google Maps.

2.3.4 Power Data from cables

Objective 2 of the FLOWERS WP2 was to compare the measured data with the modelled data. To do this, we needed to know the current being transmitted at the exact time we took our measurements. Working with the OFTOs, we obtained real-time power data for 11 of our 14 cable sites. Knowing the power and the voltage rating of the cable we were able to calculate the electric current (applying Watts Law) equation. The data supplied were for active power (megawatts, MW), ranging from the nearest second to power averaged over a certain period (e.g. 10 minutes). The time to the nearest second of the measurement recorded by the Spectramag-6 software was used to identify the correct power measurement.

2.3.5 Measured Data Handling

Time-stamped, magnetic field data from both sensors (where available) were exported from the Spectramag-6 software as microTesla (μT) peak to peak (PkPk). The data for the comparison with the simple magnetic field model used microTesla (μT) Root Mean Square (RMS) values from sensor 1. For every survey point along the transect of each power cable site, the total magnetic field around 50 Hz was dominated by readings of 49.893 Hz and 50.377 Hz, with an average of 81% of the data represented by these two frequencies (within the 48-52 Hz range). Therefore, the B-field at 50 Hz for each axis (x, y and z) was determined from:

$$B \text{ field } x_{50} = \frac{\sqrt{x_{49.893}^2 + x_{50.377}^2}}{2}$$

$$B \text{ field } y_{50} = \frac{\sqrt{y_{49.893}^2 + y_{50.377}^2}}{2}$$

$$B \text{ field } z_{50} = \frac{\sqrt{z_{49.893}^2 + z_{50.377}^2}}{2}$$

From these x, y and z values at 50 Hz the total magnetic field was calculated as:

$$\text{Total B field (PkPk)} = \sqrt{x^2 + y^2 + z^2} \mu\text{T PkPk}$$

$$\text{Total B field (Pk)} = \frac{\text{Total field (PkPk)}}{2} \mu\text{T Pk}$$

$$\text{Total B field (RMS)} = \sqrt{x^2 + y^2 + z^2} \mu\text{T RMS}$$

At each field site, the transect orientation to the buried cable was estimated. To ensure that the data were analysed perpendicular to the cable, the transect GPS readings were overlaid on the cable route map in GPS mapping software. Most transects were regarded as perpendicular if they were $<10^\circ$ deviant from the expected 90° . For transects with $>10^\circ$ the data were adjusted using the cosine trigonometric function for right-angled triangles:

$$\text{True distance to cable axis (m)} = \text{Transect point distance} \times \cos(\text{angle of deviation})$$

Furthermore, as the cables were buried, the actual linear distance to the cable itself was determined for all cables from Pythagoras' theorem:

$$\text{True distance to cable (m)} = \sqrt{(\text{distance to cable axis})^2 + (\text{cable burial depth})^2}$$

From these adjusted values, the magnetic field intensities associated with 50 Hz AC cables and their propagation with distance from the cable were represented in graphs. The software also provided a recording of the range of the overall magnetic field intensities, which includes the background fields present. The ranges were visualised graphically to illustrate how magnetic field variability changed with increasing distance from the cable.

2.3.6 Data Storage

All data were initially saved locally on the laptop used on the survey, then on secure servers, and backed up regularly to prevent data loss. The data were organised by location and date to facilitate analysis.

3. EMF Results

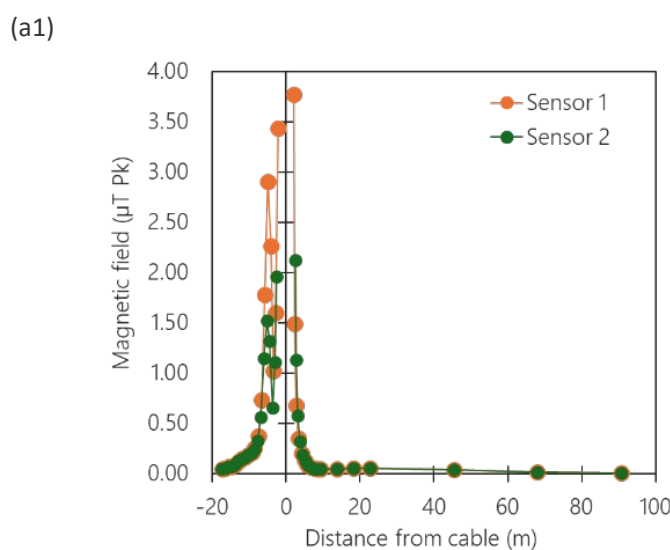
The outputs of the analysis of the relationship between individual power cable and the magnetic field are presented for each of the four geographic regions where field survey transects were undertaken. For the *in-situ* measurements of the magnetic environment, the results are displayed as zero-peak magnetic field graphs, reflecting the magnetic field intensities that organisms are likely to experience. For biological context, we include a consideration of the magnetic field measurements with regards to the knowledge on the known (to date) range of intensities of magnetic fields that has elicited responses of organisms. Furthermore, the aspects of the measurements that are most relevant to floating offshore wind are summarised.

3.1 Measurements of magnetic fields

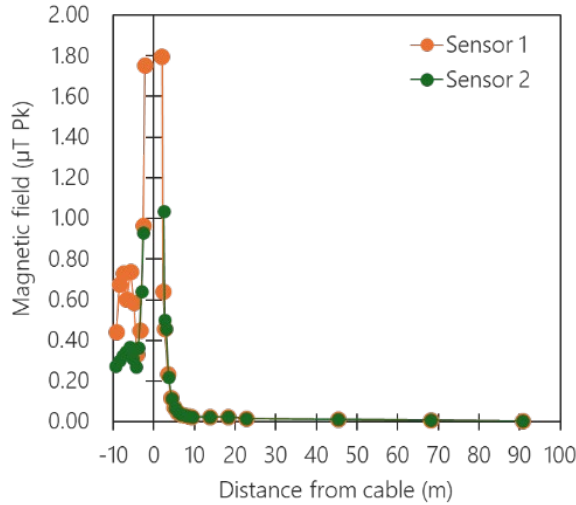
At each of the sites within each Region, the same survey methodology was used to allow an assessment of typical characteristics of the magnetic fields. The data from the two magnetometers (Sensor 1 and 2) were downloaded, corrected where required (see Section 2.3.5) and plotted in relation to the transect position.

3.1.1 Region 1 - Norfolk and the Wash

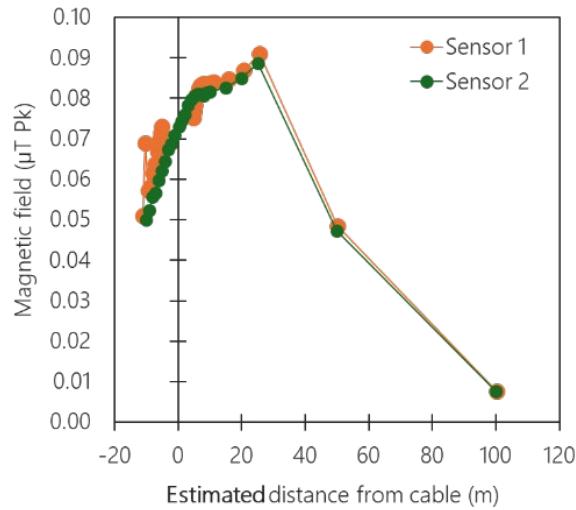
There were three sites in this region: Figure 12 (a1 and a2) 3 x 33 kV HVAC cables (measured on two separate occasions), (b) 2 x 132 kV HVAC cables and (c) 3 x 220 kV cables.



(a2)



(b)



(c)

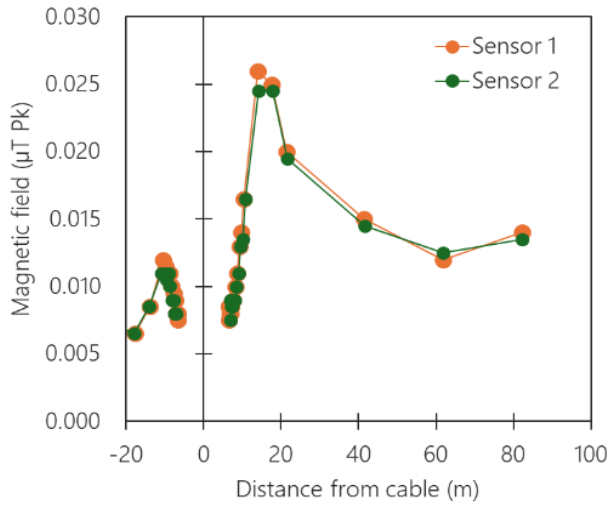


Figure 12. Measurements at export cable sites showing on the left magnetic field intensity for Sensor 1 (orange) and Sensor 2 (green) in relation to distance from the cable (at 0 m). Site (a) had 33kV cables and there were two site visits, one in July (a1) and the second in September (a2). Site (b) had 132kV cables and site (c) 220kV cables, within Region 1.

During both visits to the 33 kV site (a), the magnetic field was highest above the cable axis (Figure 12 a1 and a2). The same survey method and locations were used on both occasions. Therefore, the difference in the intensities was attributed to a difference in power generation by the wind turbines. During the sampling period, the

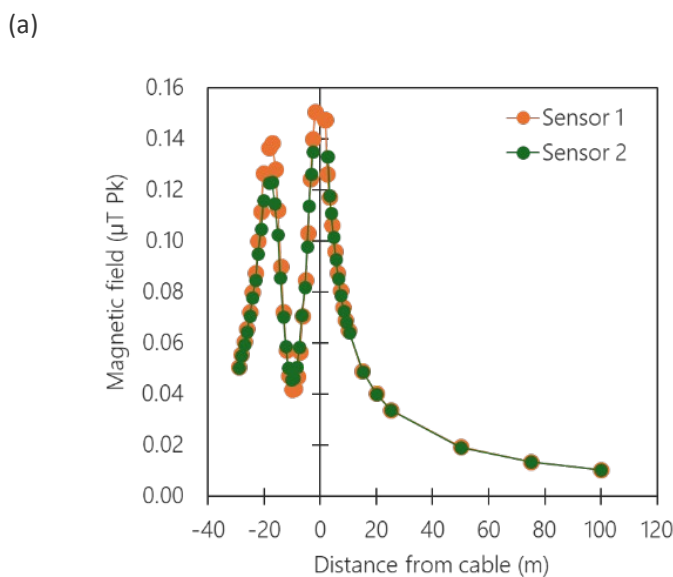
recorded power in July was 7.86 MW, whereas in Sept it was 2.18 MW. For both surveys of the 33 kV cable, the magnetic field intensity decreased rapidly with distance (Figure 12(a1)).

The site in Figure 12b was a steep shingle beach with the cable HDD starting from around the low water mark under the beach through a deep pipe. It was not possible to determine the depth from as-built details; therefore, we estimated the burial depth as between 2 and 5 m. Based on the measurements, the estimated centre of the cable was not correctly located during our survey, as the post-survey highest reading did not correspond to the zero metre point (centre of cable; Figure 11b). Furthermore, the drop off with distance was not as rapid as at the 33 kV site in Region 1. It was noted that at this site, there were two cables from one wind farm and nearby another two cables from a different offshore wind farm. As we did not locate the focal cable correctly, we may have been detecting the influence of other cables. Nevertheless, the 50 Hz magnetic field was measured at the beach surface and these magnetic field levels were within the detection zone, shown by the blue shading.

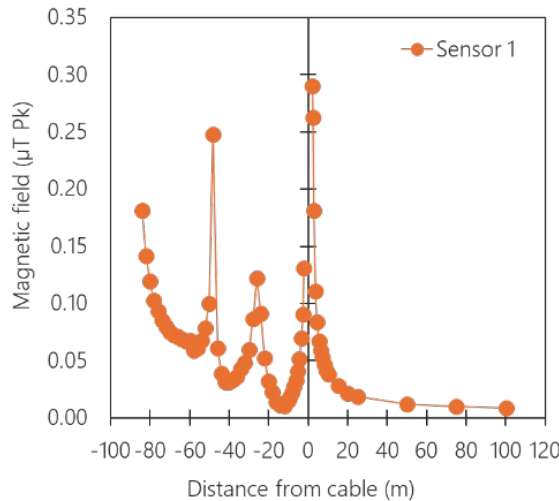
At the 220 kV site, the magnetic field was measured but at very low intensity (Figure 11c). This can be attributed to low winds leading to low power transmission on this day, estimated at less than 10% of the maximum on the day and time we visited. The HDD cables were also estimated to be at a burial depth between 5.5 and 7 m. As the magnetic field was low intensity, we were not able to find the cable axis, and therefore, the peak based on the measurements was 15-20 m from our zero point.

3.1.2 Region 2 - Outer Thames

There were three HVAC sites in Region 2: one with 2 x 132 kV HVAC cables measured by both Sensor 1 and 2 (Figure 13a), a second site with 4 x 150 kV HVAC cables (Figure 13b), and a third with 2 x 132 kV HVAC cables (Figure 13c). During the surveys of the second and third site, sensor 2 was not working correctly, therefore Figure 13b and c show only Sensor 1 data.



(b)



(c)

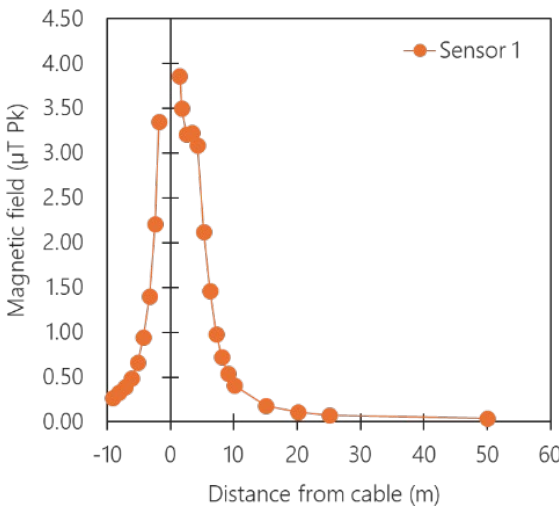


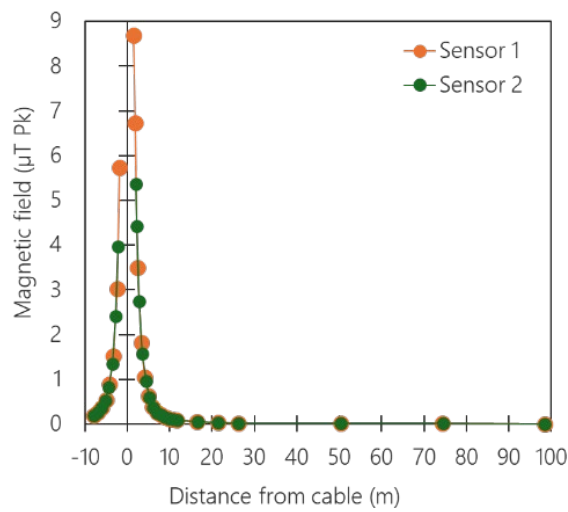
Figure 13. Measurements at two 132 kV sites and a 150 kV site within Region 2 shown on the left, with magnetic field intensity for Sensor 1 (orange) and Sensor 2 (green) in relation to distance from the cable (at 0 m). Note: at sites (b) and (c) Sensor 2 was not working properly; therefore, data were removed.

Peak intensity of the magnetic field was directly above the cable axis, and the intensity dropped off with distance for all Region 2 sites. Figure 13a and b also display the peaks observed for the other cables at the respective sites. With multiple cables the overall spatial extent of the magnetic fields in the environment was related to the number of cables and the intensity of the magnetic field produced by the adjacent cables. In the context of the environment that an animal would experience, the magnetic field is raised over the spatial extent of all the cables present. The magnetic field range appeared to be greater nearer to the cable for each site, although the difference was most pronounced at site (c).

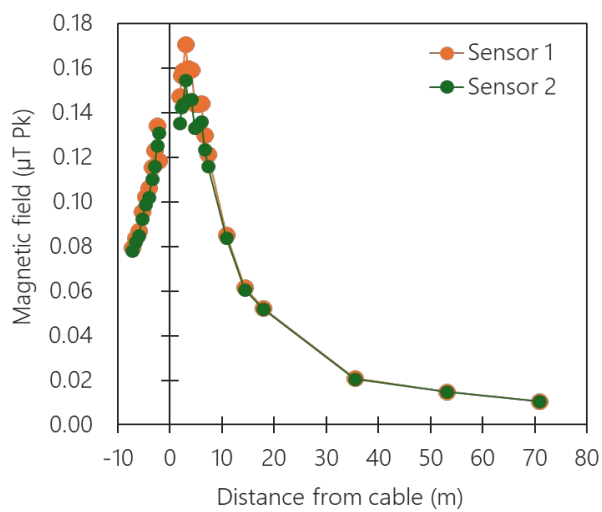
3.1.3 Region 3 - Liverpool Bay

There were four sites in Region 3: (a) 1 x 132 kV HVAC cables, (b) 1 x 132 kV HVAC cables, (c) 2 x 220 kV HVAC, and (c) 4 x 132 kV HVAC cables.

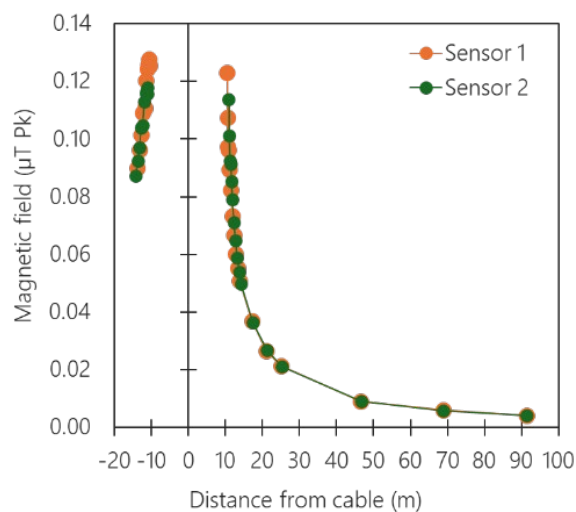
(a)



(b)



(c)



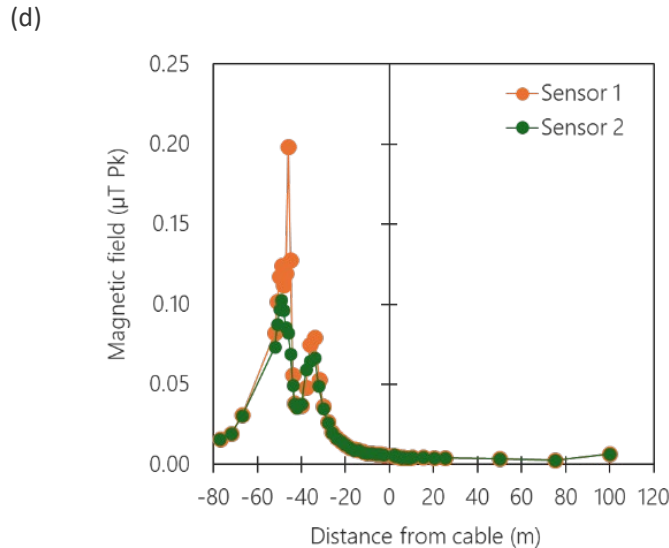
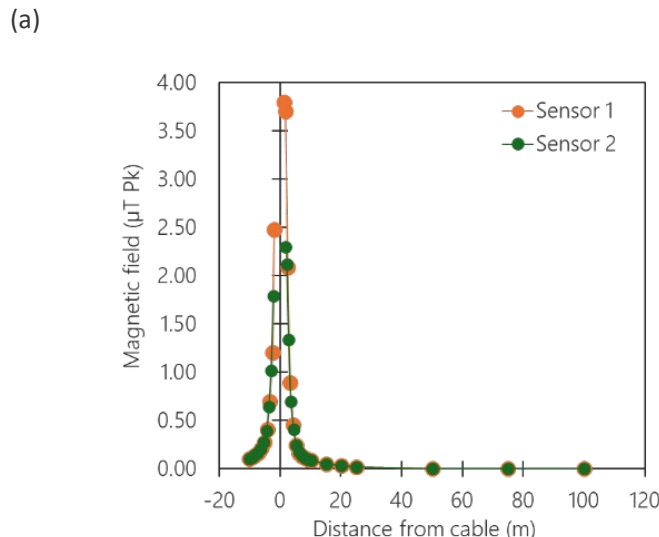


Figure 14. Measurements at three 132 kV sites and a 220 kV site within Region 3. (a) 1 x 132 kV HVAC cables, (b) 1 x 132 kV HVAC cables, (c) 2 x 220 kV HVAC, and (c) 4 x 132 kV HVAC cables. Magnetic field intensity for Sensor 1 (orange) and Sensor 2 (green) in relation to distance from the cable (at 0 m).

In Region 3, the first and second sites (Figure 14a and b) were single cables with the peak intensity nearest the cable axis. The drop-off with distance appears less rapid at site (b), however, the scale should be noted as the magnetic field intensities were very much lower than at site (a). For all sites in Region 3, the magnetic field intensity above the lowest detection threshold extended over tens of metres. At site (c), the export cables were buried via HDD to an estimated depth of 10.5 m based on the as-built data; therefore, we obtained no readings of the cable less than 10m. At site (d), the power data showed that different levels of power were being transmitted through the four different cables. The selected cable appeared to be operating at a relatively low power level, while two adjacent cables located approximately 34 m and 49 m away were transmitting at higher intensities; Figure 14 (d). This variation in power output between the cables was reflected in the measured magnetic field gradients across the transect.

3.1.4 Region 4 - North Scotland

There were two HVAC sites in this region: (a) 2 x 220 kV HVAC cables, (b) 3 x 220 kV HVAC cables.



(b)

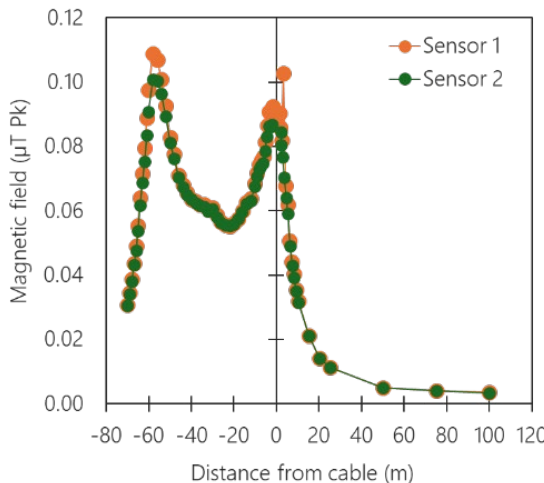


Figure 15. Measurements at two 132 kV export cable sites within Region 4 are shown on the left, with magnetic field intensity for Sensor 1 (orange) and Sensor 2 (green) in relation to distance from the cable (at 0 m).

In Region 4, at site (a) one of the cables was measured, which displayed a typical rapid decline in magnetic field intensity associated with a single cable. The other export cable was located at distance from the measurement transect. In contrast, site (b) had three cables spaced approximately 25 m apart, resulting in a more complex magnetic environment at the measurement location. The extent of the magnetic field was over several tens of metres, most likely due to interactions between the EMFs generated by each of the 220 kV cables.

3.1.5 Interconnectors

The focus of the FLOWERS WP2 project was operational offshore wind export cable landfall sites; however, during two of the site visits, we also measured magnetic fields of nearby interconnector cables. In Region 2, a single 320 kV HVDC cable (Figure 16a), and in Region 4, a single 400 kV HVDC cable (Figure 16b) were measured. HVDC cables will interact directly with the Earth's local geomagnetic field. The resultant magnetic field environment will depend on the cable's orientation to the geomagnetic field. Figure 16a and b show the resultant DC magnetic field at the two sites, with the maximum and minimum intensity being very similar, shown by the coincident points on the graph. In Region 2 (Figure 16a), the cable was north-south oriented and the measurements showed a maximum reduction of approximately 5 μ T in the local magnetic field, with some reduction extending approximately 20 m on either side of the cable (Figure 16a). The red line indicates the background DC geomagnetic field intensity for the site, estimated from the International Geomagnetic Reference Field (IGRF) Calculator (British Geological Society). In Region 4 (Figure 16), the cable was east-west oriented, and the resultant magnetic field intensity reached over 100 μ T at an estimated 1.5 m from the buried cable, with the magnetic field intensity raised over a relatively short 3 m on either side of the cable axis.

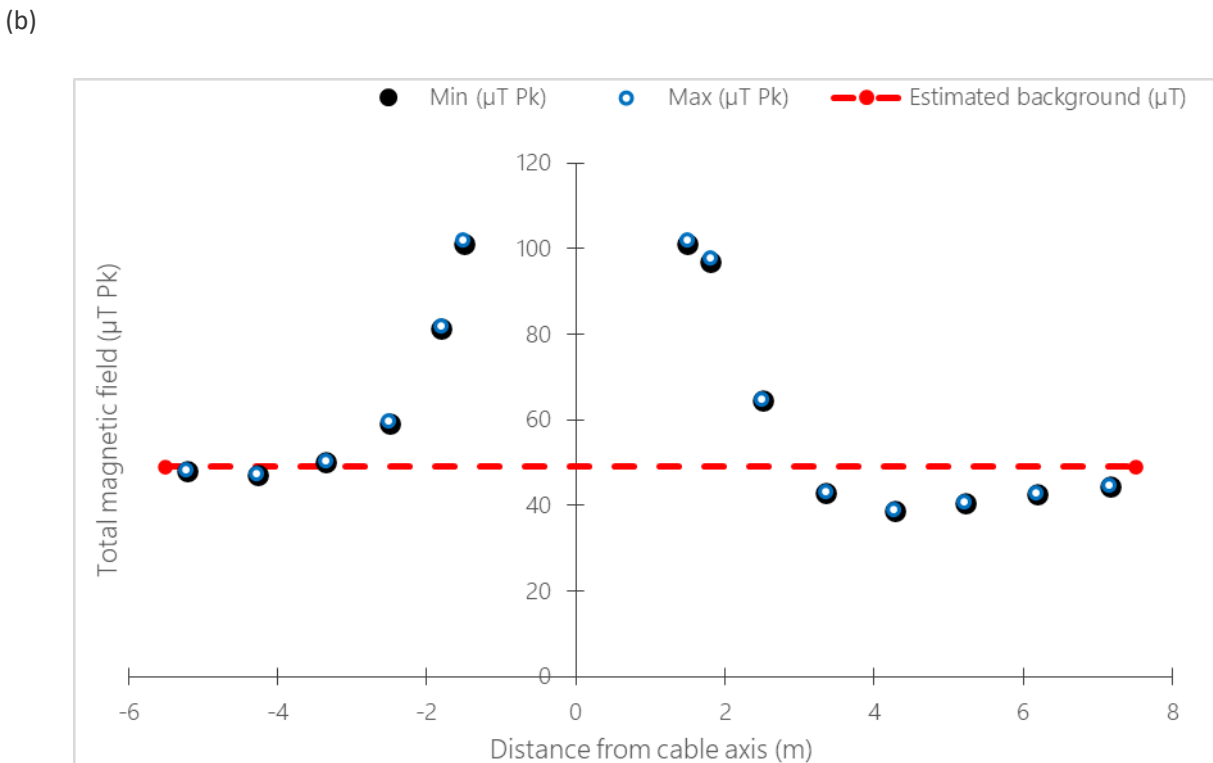
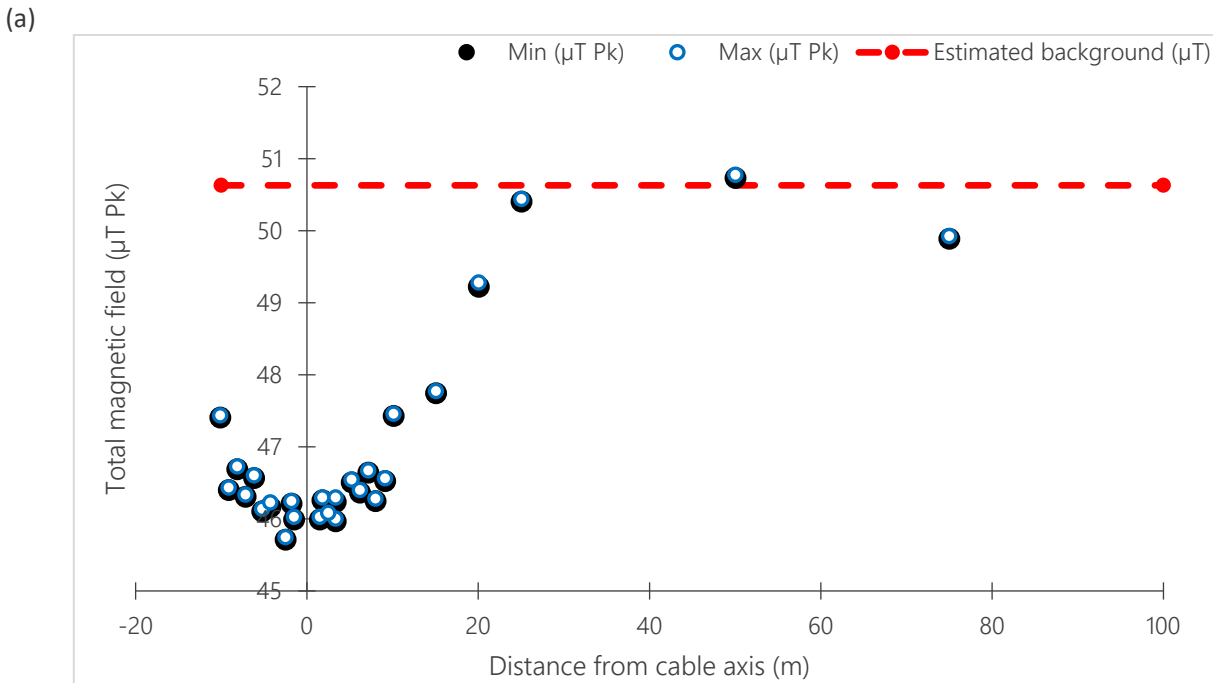


Figure 16. Field measurements for two interconnector sites within (a) Region 2 and (b) Region 4, showing the overall magnetic field intensity maximum (blue and white circles) and minimum recordings (black circles) in relation to distance from the cable (at 0 m). The red broken line shows the background geomagnetic field intensity for the location, based on the International Geomagnetic Reference Field (IGRF) Calculator via the British Geological Society.

3.1.6 Comparing sensor 1 and 2

Two identical magnetometers were used to verify that the relationship between the magnetic field intensity and distance was consistent, as demonstrated in the HVAC plots from Section 3.1.1 to 3.1.4. Using two sensors also

enabled confirmation that the magnetic fields being measured were not an artifact of a single magnetometer being used (Figure 17).

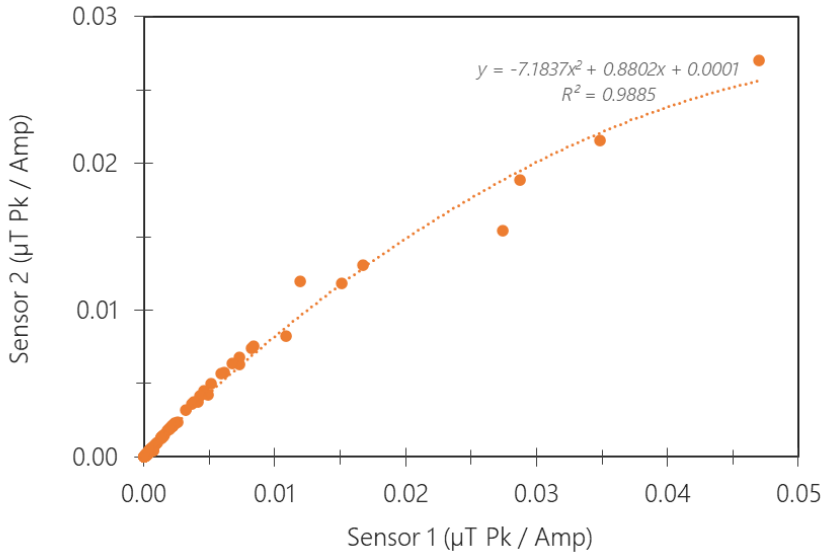


Figure 17. Relationship between Sensor 1 and Sensor 2, standardised for the current generating the measured magnetic field.

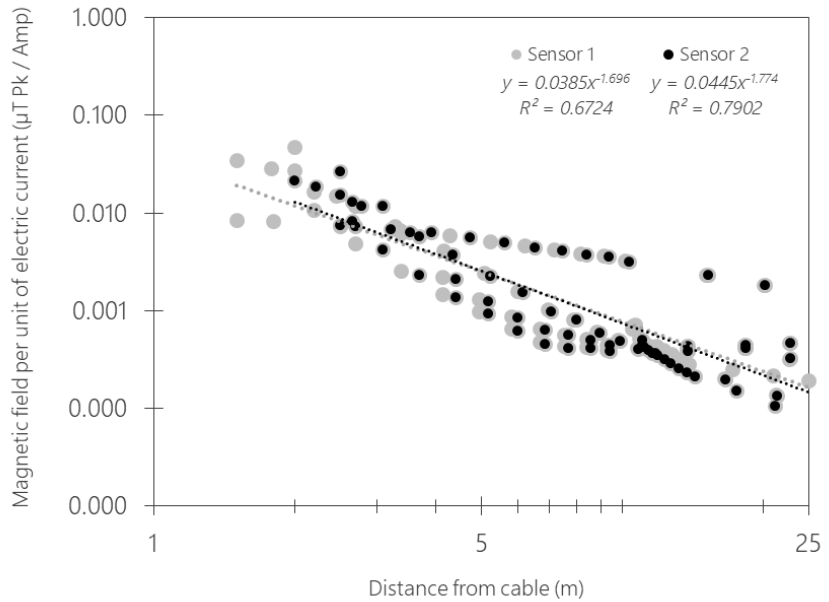


Figure 18. Relationship between the magnetic field measured and distance from cable, standardised per unit electrical current, for five cable surveys (2 x 33 kV, 2 x 132 kV and 1 x 220 kV). Enlarged grey points highlight coincident black and grey data values.

Whilst the relationship between the two Sensors appeared consistent, there were differences nearer to the cable (Figure 17). Figure 17 shows that the overall relationship between the two sensor measurements was closely matched (see grey and black trendlines and match between the data points) when standardised by the amount of electrical current creating the magnetic field. However, nearer the cable the relationship is less clear. This pattern is likely to be a result of variations in cable characteristics and the complexity of the magnetic fields closer to the cable.

3.1.7 Biological context of magnetic field measurements

The ability to detect gradients in magnetic fields and electric fields in the marine environment is known to exist for a wide range of taxa from bacteria to mammals (Albert et al., 2020; Gill and Desender 2020; Hutchison and Gill, 2025; Nyqvist et al., 2020). Whilst the sensory mechanisms for detecting EMFs and the intensities and frequencies of the fields that result in a response by organisms are still debated, the evidence highlights that a wide range of species across many taxa do respond. Such responses can be behavioural, physiological, biochemical, developmental, or genetic regardless of whether the organism has sensory apparatus that has been identified (Albert et al., 2020; Gill and Desender 2020; Hutchison and Gill, 2025). Therefore, it is important to consider how the knowledge gained from measuring the magnetic field environment associated with subsea power cables feeds into the assessment of the potential for interaction with organisms.

In general, the DC and AC magnetic field intensities that are known to be detectable range from nT (Amphipods, eels and cetacean examples) to 10s of mT (teleost fish, crustaceans; Normandeau et al. 2011; Nyqvist et al. 2020). The magnetoreceptive animals respond to the magnetic field gradient and inclination with respect to the background geomagnetic field. For the associated electric fields, the known intensities range from low $\mu\text{V/m}$ (e.g. elasmobranchs, lampreys) to 10s V/m (crustaceans and molluscs, Normandeau et al. 2011; Nyqvist et al. 2020; England and Robert, 2022). It should be highlighted that much of the knowledge on detection and response of organisms to magnetic (and electric) fields is patchy (Hutchison et al. 2020b), and studies at the higher levels (i.e. high μT up to mT) often used in laboratory studies are much higher than the EMFs emitted by subsea power cables at maximum power (see green modelled data in Figure 19).

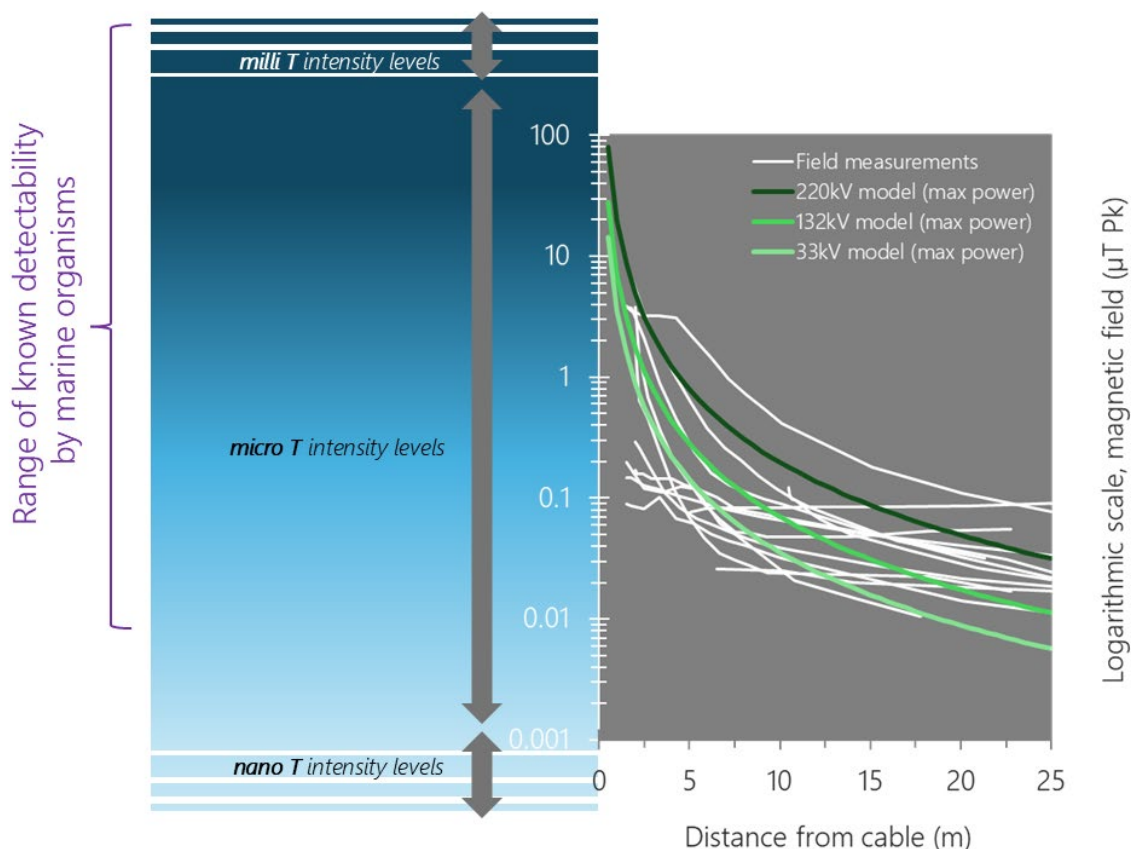


Figure 19. The ability of marine organisms to detect magnetic fields is represented on the left, based on their known range of detectability, for the purposes of comparison to the measured and modelled magnetic fields from HVAC cables, on the right. The range of magnetic field intensities is from nanotesla to milliTesla. Magnetic fields are presented with distance from each cable (up to 25m) measured at multiple export cable sites and overlaid with models of three typical HVAC export cables (33kV, 132kV and 220k) at maximum power. The magnetic field intensities measured were within the microTesla range, which overlaps with the known range of detectability by marine organisms.

In Figure 19 the measurements from Section 3.1.1-3.1.4, have been compiled to be compared with the known range of magnetic field intensities that are associated with responses (reviewed by Albert et al. 2020; Gill and Desender 2020; Hutchison and Gill, 2025; Normandeau et al. 2013; Nyqvist et al. 2020). At the minimum level (nT), the evidence of responses by species is sparse, whereas within the μ T and mT range there are many studies across a wide range of taxa. The range of known detectability shown in Figure 19 indicates the magnetic fields that were measured for typical export cables were within the range of detection or response of most organism groups that have been studied (from approximately 0.005 μ T to mT magnetic field intensities). Furthermore, the addition of the modelled magnetic fields at maximum power transmission level for typical export cables in Figure 19, highlights that the magnetic field intensities associated with variable wind power generation overlap with the range of known detectability by species. Whilst we measured at intervals up to 100m away from the cable axis, the magnetic field intensities up to 25m were used to compare with known detectability by species. We had fewer sample points beyond 25m and the measurements all reduced to low levels that are at the limit of known detectability (e.g. Figure 13c; Figure 14a). If there were more than one cable, then the magnetic fields interacted and kept the magnetic field intensities higher and within the range of known detectability (e.g. Figure 13a; Figure 15b), which would increase the spatial extent of the EMFs associated with a cable(s) corridor.

It is important to note that detection and any subsequent response of an organism to magnetic fields does not mean that there is any impact associated with the encounter. However, it provides clear reasoning with regard to the need to understand the encounter between organisms and SPC EMFs further, which is dealt with in the subsequent sections of WP2.

A further point of note is that where EMFs have been considered within an environmental assessment context, modelling of the EMF is undertaken for maximum power loads. The outputs are often graphically represented as the magnetic field (and sometimes electric field) intensity plotted against horizontal distance from the cable axis (i.e. along the seabed surface). Several examples are shown in Section 2.1, Figure 4. These models are then used to represent the EMFs in the environment that receptors may encounter. Based on the *in-situ* measurements, the propagation of the magnetic fields appears not to decrease as rapidly as the previous modelling indicates. For greater confidence in the environmental assessment of EMFs, it should be ensured that the EMF environment is representative of what the organisms will encounter.

3.2 Comparison of measured and modelled magnetic fields

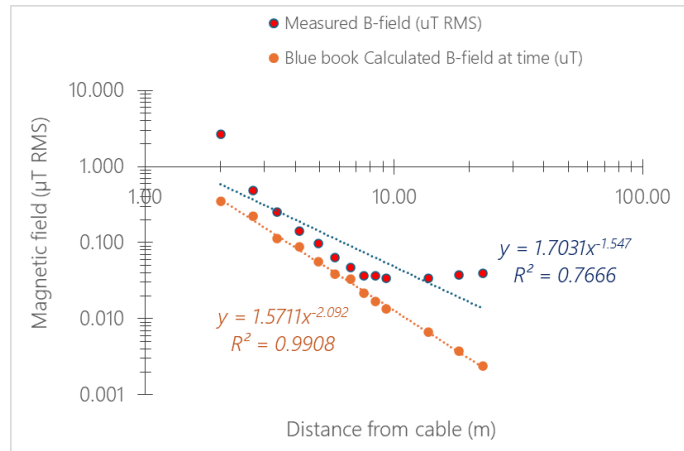
3.2.1 Modelled magnetic field using power data

To enable comparison between the measured and modelled magnetic fields, it was essential to obtain the electrical current of the cable at the time of measurement and then include these values into the models. We used export power data supplied by cable operators, where available, to determine the electrical current in a single cable when we were measuring the magnetic field. If there was more than one cable, it was assumed that the power was equally divided between the cables; however, in some cases power data were specific to each cable. Furthermore, the cables' characteristics, the configuration of the cable cores and information on the burial depth were required to enable a suitable comparison to be undertaken. Unfortunately, not all these data were available for all sites.

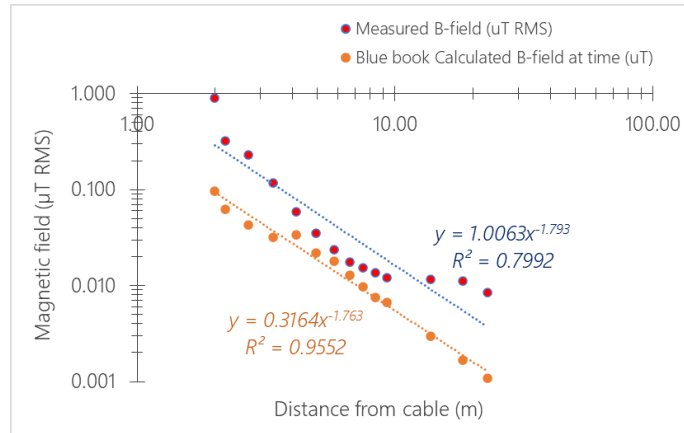
Based on these requirements, a sub-sample of four sites (with one site measured on two occasions), with different cable types, was chosen for the comparison. Sites with missing/incomplete data, uncertainty about depth of burial, or with interference from adjacent cables, were omitted.

The comparison between the modelled and measured data was log-log plotted using RMS values of the magnetic field for the specific current in the cable at the time of measurement (Figure 20a-e). All sites showed consistent discrepancies between measured and modelled relationships. The models predicted that the magnetic field intensity would decrease at approximately $1/r^2$. However, the measured data showed a more gradual decline, suggesting a deviation from the model. The strength of the relationship was high for the models (as represented by the regression coefficient R^2 in the log-log plots). The relationship between the measured magnetic field intensity and the distance from the cable was more variable and, in some cases, it appears that there was a shift in the relationship around the 10 m point (see Figure 20b, c, d, and e).

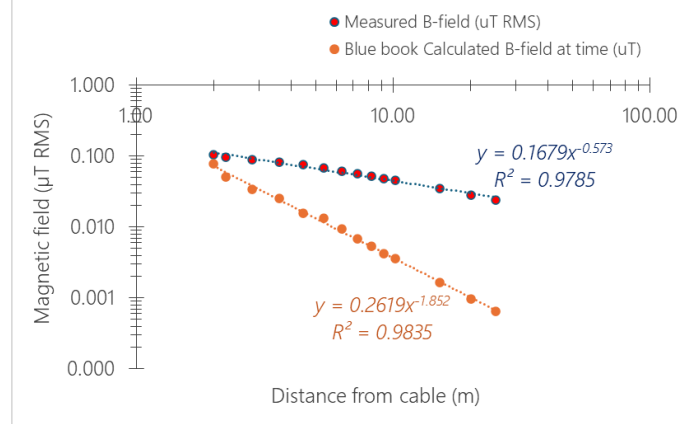
(a) Region 1 - Norfolk and The Wash



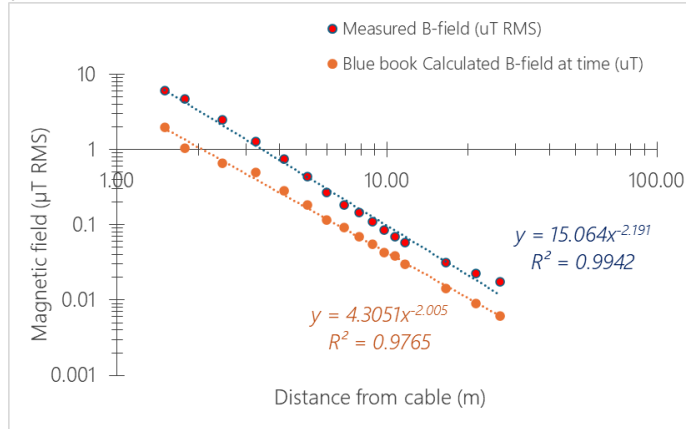
(b) Region 1 - Norfolk and The Wash



(c) Region 2 - Outer Thames



(d) Region 3 - Liverpool Bay



(e) Region 3 - Liverpool Bay

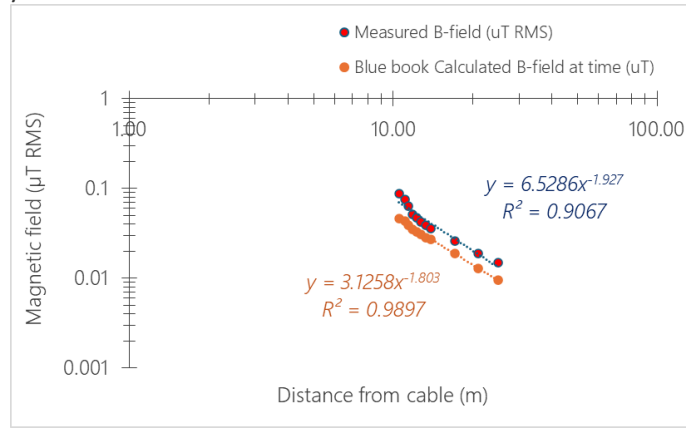


Figure 20. Log-log comparison of measured and modelled data at four different sites. (a) and (b) Norfolk and The Wash (33 kV), (c) Outer Thames (132 kV), (d) Liverpool Bay (132 kV), and (e) Liverpool Bay (220kV). Dotted lines show best fitting curve with equation of the line and the coefficient of determination (R^2).

The main outputs to note for Objective 2 are:

- Magnetic fields measured in the environment differ from basic model estimates.
- The measured magnetic fields were higher than that of the models and propagate further with distance from the cable.
- Not all of the sites were used for the comparison of measured and modelled magnetic fields because essential cable data to input into the modelling were not always available.
- The presence of multiple cables within an existing cable corridor increased the spatial extent of the measured magnetic fields.
- The *in situ* magnetic field intensities showed overlap with the known range of intensities that can be detected by species. We used a conservative approach of applying the range from low intensity magnetic fields (approximating 0.001 µT) to 10s of mT, noting the upper and lower intensities are based on limited data from a small number of species. In future, the detection ranges of the specific species of interest should be used, where available, when assessing the potential exposure to EMFs.

3.3.1 Floating offshore wind cable considerations

- Based on the current modelling used and the measurements from fixed offshore wind export cables there is a need to develop the modelling further to be more representative, particularly at distance. As the EMFs from subsea cables either buried or in the water column share the same properties the improvement in modelling is relevant to floating and fixed cables.
- There is little knowledge of EMFs of dynamic cables and in particular near to the surface of the cable (apart from modelling predictions). Therefore, there some validation and further study will be required to ensure the knowledge moves towards an accepted modelling approach.

4. Species occurrence and distribution (Objective 3)

To consider the potential for receptor species to encounter subsea power cable EMFs, it is necessary to have knowledge of their occurrence and distribution in the geographical area of interest. For some receptors there are spatial occurrence data available (e.g. [Cefas Spatial Hub – GeoFISH Portal](#)). However, the amount of data available will vary depending on the species and the location, particularly in areas where there are spatially explicit data gaps. In these cases where more data are required, species distribution estimation can be used to predict occurrence and spatial distribution (Couce *et al.* 2025).

4.1 Focal Species and Species Distribution

As the method for determining the likelihood of encounter with subsea cable EMFs needed to be generally applicable, we chose three focal species to represent groups of species with different attributes. The selection of the focal species was based on: the best available fish species spatial distribution data to cover regions where EMF field surveys were conducted (Table 2; Figure 7), the most recent scientific knowledge on EM-sensitive species, and consultations with the Project Advisory Group (PAG). The species chosen were basking shark (*Cetorhinus maximus*), European seabass (*Dicentrarchus labrax*), and thornback ray (*Raja clavata*). These species represent a range of life histories, have conservation or fishing status within UK waters, and are either demonstrated to have EM-receptive capabilities or are proposed to use electric or magnetic field cues in the environment (Table 2).

Table 2. List of the focal species and their attributes, selected for spatial occurrence and distribution analysis within EMF fieldwork regions.

Category	Selection Criteria			Species
Benthic	Taxonomic group Ecology Life stage Status EM-sense	Elasmobranch Resident / seasonal migrations Adult Commercial and recreational fishing importance Electromagnetic sense (induction)		Thornback ray (<i>Raja clavata</i>)
Pelagic	Taxonomic group Ecology Life stage Status EM-sense	Finfish Widely distributed Adult Commercial and recreational fishing importance Orientation to geomagnetic field in juveniles (proposed)		European seabass (<i>Dicentrarchus labrax</i>)
Migratory – large scale	Taxonomic group Ecology Life stage Status EM-sense	Elasmobranch Epipelagic and Migratory – regional scale Adult Conservation importance Electromagnetic sense (induction)		Basking shark (<i>Cetorhinus maximus</i>)

Species distribution modelling outputs undertaken by Cefas within UK waters for a previous project were available and provided spatial data for the basking shark, European seabass and thornback ray (Couce *et al.*, 2025; Townhill *et al.*, 2023). The distributions were based on occurrence records for the period 2005-2014. Data had been modelled using an ensemble of Habitat Suitability models, which compared conditions at sites where a species is known to be present with sites where it is known to be absent (Couce *et al.*, 2025). Species occurrence data sources included the International Council for Exploration of the Sea (ICES) Groundfish Survey Monitoring and Assessment Data Products (DATRAS) for the North-east Atlantic Area (Moriarty *et al.*, 2017), which contains all the groundfish survey datasets uploaded to the ICES system, and from the Ocean Biogeographic Information System (OBIS) online portal (<https://obis.org/>). Additional data were included for the basking shark from the Global Biodiversity Information Facility (GBIF, 2021) and the Basking Shark Watch Database 1987-2020 managed by the Shark Trust, under licence from the Marine Conservation Society, and by Colin Speedie and Wave Action (Austin *et al.*, 2019). Data were projected onto a 0.25° x 0.25° study grid, and cells with data were classed as “presence” sites, while remaining cells were classed as “absence” sites.

The species distribution models used the Intergovernmental Panel on Climate Change (IPCC) ‘Representative Concentration Pathways’ (RCPs) climate projections for 20-year periods to 2070 for the European seabass and thornback ray (Townhill *et al.*, 2023), and for each decade to 2100 for basking shark (Couce *et al.*, 2025). Here we used the training data for the decade 2020 to represent the species’ current habitat suitability in UK waters.

4.2 Spatial data handling in GIS

Data from the Crown Estate were obtained for Offshore Wind Cable Agreements (England, Wales and Northern Ireland) and Offshore Wind Site Agreements (England, Wales and Northern Ireland). Based on the field measurements of subsea power cables (SPCs), we estimated the extent of magnetic fields associated with SPCs to be in the order of tens of metres, owing to a combination of the power being transmitted, the type of cable and the number of export cables (see Section 3.1). Under the assumption that the export cables may be located anywhere within the cable corridors, and inter-array cables may be present anywhere within the offshore wind farm licence areas, we applied 50 m buffers to each data layer to spatially represent electromagnetic field zones. This buffer zone was selected to represent the modal extent of magnetic field from the data from all export cable sites we measured, which was above the lowest level of detection reported in the literature (see Section 3.1.7.; Figure 19)

The offshore wind footprints and cable routes with the 50 m buffer zone were overlayed onto habitat suitability layers for each of the focal species to determine spatial overlap. This represents a key step in determining the likelihood of encounter between each species with potential EMF zones. All spatial analysis was undertaken using ArcGIS Pro (version 3.2.2).

The GIS outputs in the form of gridded squares are set out using the approach below according to the categories of benthic, pelagic and migratory species, which were used to illustrate a generally applicable stepwise approach to determining the likelihood of encounter. It should be noted that white areas occur in the spatial outputs, and these are indicative of the absence of data (see Figures 21-23). This is a known limitation of the Habitat Suitability models available, which use data from offshore surveys and therefore do not adequately provide habitat suitability data estimates for nearshore coastal waters.

4.3 Stepwise approach to determining the likelihood of encounter

The stepwise approach applied uses the example of the habitat suitability and EMF zone GIS outputs, however it is set out here as a general approach:

- i. Design a table based on the GIS coloured grid square scale and assign a weighting to each row (Table 3).

Note 1: The number of rows can be adjusted according to the GIS categorisation chosen. The minimum number of categories would be three: 1) blank-no data, 2) species absent data, 3) species present data.

Note 2: It is suggested that, for simplicity and to maintain objectivity, the weighting uses the same increment between category weighting values, unless more specific evidence can justify differential weighting. If the latter, then the evidence source must be provided.

- ii. Design a second table, which incorporates the grid categories and their weighting (from Table 3). To this second table add the count of all GIS grid squares per category in the defined area (e.g. Table 4, column C).

Note: some areas coincident with cable EMF zones have no data, particularly near the coast, as exemplified in Figures 19, 20 and 21. Such blank grid squares are included in the total count to highlight the absence of data.

- iii. Calculate the total count of each coloured grid square that intersects with some part of the EMF cable zones (Table 4, column D).

Note: for simplicity, only count grid squares that represent over half of the aquatic habitat in a grid square).

- iv. For each offshore wind development EMF footprint (i.e. the EMF zone of the turbine array and the export cable route), count the number of grid squares per category that intersect with the cable EMF zone and add to a separate column per offshore development (Table 4, columns Fi, Fii etc).

Note: for simplicity, only count offshore developments that have grid squares with data for the whole extent of their EMF footprint.

- v. To provide an indication of the cumulative likelihood of encounter of a receptor with SPC EMF zones for a defined region, divide the count of each of the coloured grid squares (step iii) by the total number of grid squares (step ii) to give the proportion of overlap between coloured grid squares and EMF cable zones (Table 4, column E).
- vi. Assign categories of likelihood of encounter based on weighted proportions: here we used a) <25% = low; b) 25-50% = low-medium; c) 50-75% = medium-high; or d) >75% = high.
- vii. Assign confidence level for the data set used based on the proportion of spatial grid squares with data in relation to the total number of grid squares in the region (i.e. including all grid squares including no data; see Table 4).
- viii. If overlap confirmed, move on to the next stage.

Table 3. Weighting to apply to GIS species data grid square categories (the example here relates to habitat suitability). Note: The number of rows can be adjusted according to the GIS categorisation chosen, to ensure the best representation of the data.

Grid box proportion categories (e.g.)	Grid square coverage definition (e.g. Habitat Suitability)	Weighting
Blank	No species-related data found	n/a
0 - 0.19	Very low	0.2
0.2 - 0.39	Low	0.4
0.4 – 0.59	Medium	0.6
0.6 – 0.79	High	0.8
0.8 – 1.0	Full / Complete	1.0

Table 4. A table template for compiling data to determine the likelihood of 2D spatial overlap (per development and/or defined region). The blue cells in the table are the weighted proportions on which to apply criteria for the 2D likelihood of encountering the EMF zones for the defined region (column E) or each offshore wind development (columns Gi, Gii, Giii, etc). The green cell represents the spatial confidence of the data for the region based on the green table categories.

The stepwise approach developed in this section and the table templates were applied to the focal species that were defined in Table 2 to assess the two-dimensional (2D) overlap with power cable EMFs. We started with the thornback ray as its benthic habitat association in coastal and offshore waters suggests there could be a high likelihood of encounter with magnetic fields from cabling along the seabed.

4.3.1 Thornback ray - benthic species

The habitat suitability for the benthic Thornback ray was high across most of the mapped area in Region 2 (Figure 21), as indicated by the dark blue gridded squares that dominate in this region. The EMF cable zones and OSW footprints are also coincident with the higher categories of habitat suitability across most of the area (Figure 21). Therefore, the likelihood of encountering SPC magnetic fields in this region was assessed to be medium-high with a high level of confidence (Table 5). For each of the offshore wind development EMF footprints, the likelihood of encounter was assessed to be high as they all overlapped with high category for habitat suitability (i.e. dark blue grid squares; Table 5).

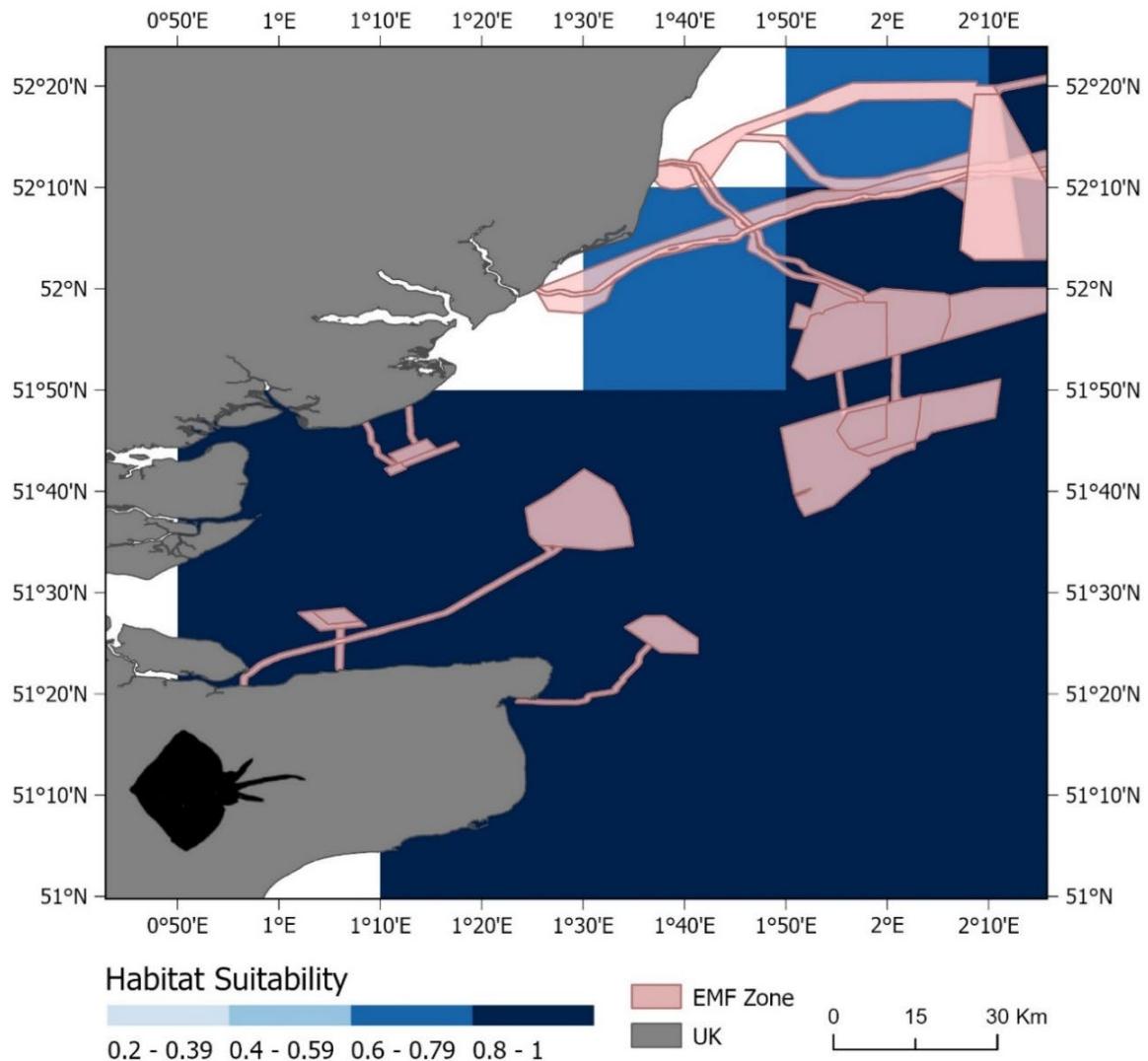


Figure 21. Overlay of thornback ray habitat suitability and fixed offshore wind farm EMFs zone footprints (including the export cable route) in Region 2. The darker the blue square, the more suitable the habitat associated with the species. The pink areas represent the offshore wind installation footprint with the 50 m EMF zone relating to the extent of the magnetic field in the marine environment for the whole offshore wind infrastructure development.

Table 5. Likelihood of encounter for the benthic thornback ray determined from 2D spatial overlap assessment of species occurrence and EMFs zones. Categories are: a) <25% = low; b) 25-50% = low-medium; c) 50-75% = medium-high; or d) >75% = high. Confidence level is based on the proportion of spatial grid squares with data in relation to the total number of grid squares in the region (i.e. no data; see Likelihood of spatial overlap data Table 4). .

A	B	C	D	E	F							G						
					Count of grid cells overlapping cable EMF zone for each offshore development							Weighted proportion of grid cell overlap with EMF zones for each offshore development = $(F_x / F_{x\text{total}}) * B$						
					i	ii	iii	iv	v	vi	vii	i	ii	iii	iv	v	vi	vii
Blank		2		0.00	0	0						0.00	0.00	0.00	0.00	0.00	0.00	0.00
0.01- 0.19	0.2			0.00								0.00	0.00	0.00	0.00	0.00	0.00	0.00
0.2 - 0.39	0.4			0.00								0.00	0.00	0.00	0.00	0.00	0.00	0.00
0.4 – 0.59	0.6			0.00								0.00	0.00	0.00	0.00	0.00	0.00	0.00
0.6 – 0.79	0.8	2	2	0.11	1	2	1					0.80	0.53	0.27	0.00	0.00	0.00	0.00
0.8 – 1.0	1	12	8	0.57	1	2	2	4	1	2	0.00	0.33	0.67	1.00	1.00	1.00	1.00	1.00
Total		14	10	0.69	1	3	3	2	4	1	2	0.80	0.87	0.93	1.00	1.00	1.00	1.00
	Total # grids cells	16																
	% data available	87.5																

Spatial confidence level - Based on grid squares with data and without	
Low	<25%
Low-medium	25-50%
Medium-high	50-75%
High	>75%

4.3.2 European Seabass - Pelagic species

The habitat suitability for the pelagic European seabass was variable across the region (Figure). The mid-blue coloured grid squares dominate in this region, and the cable EMF zones and OSW footprints are coincident with different categories of habitat suitability across the area. Therefore, the 2D likelihood of encountering SPC EMFs in this region was assessed to be medium-high with a high level of confidence (Table 5). For each of the individual offshore wind development EMF footprints, the 2D likelihood of encounter was assessed to be medium-high for most, as they overlapped with different categories of habitat suitability (Table 6). The confidence level was assigned as high because there were data available for most of the grid squares. However, some offshore wind developments were not included in the individual assessment as they had blank grid squares (no data) for parts of their footprint (Figure 20). One aspect of the 2D approach to data overlap is that pelagic species will vary in their position in the water column, which would reduce the 2D likelihood of encounter (this aspect is addressed later in Sections 4.3.5 and 4.3.6). However, the simple 2D overlap assessment is a necessary step to determine if the focal species spatial distribution would bring them into the area where subsea power cables are located. If there is no 2D overlap, then there is no need to consider the greater detail of depth of occurrence.

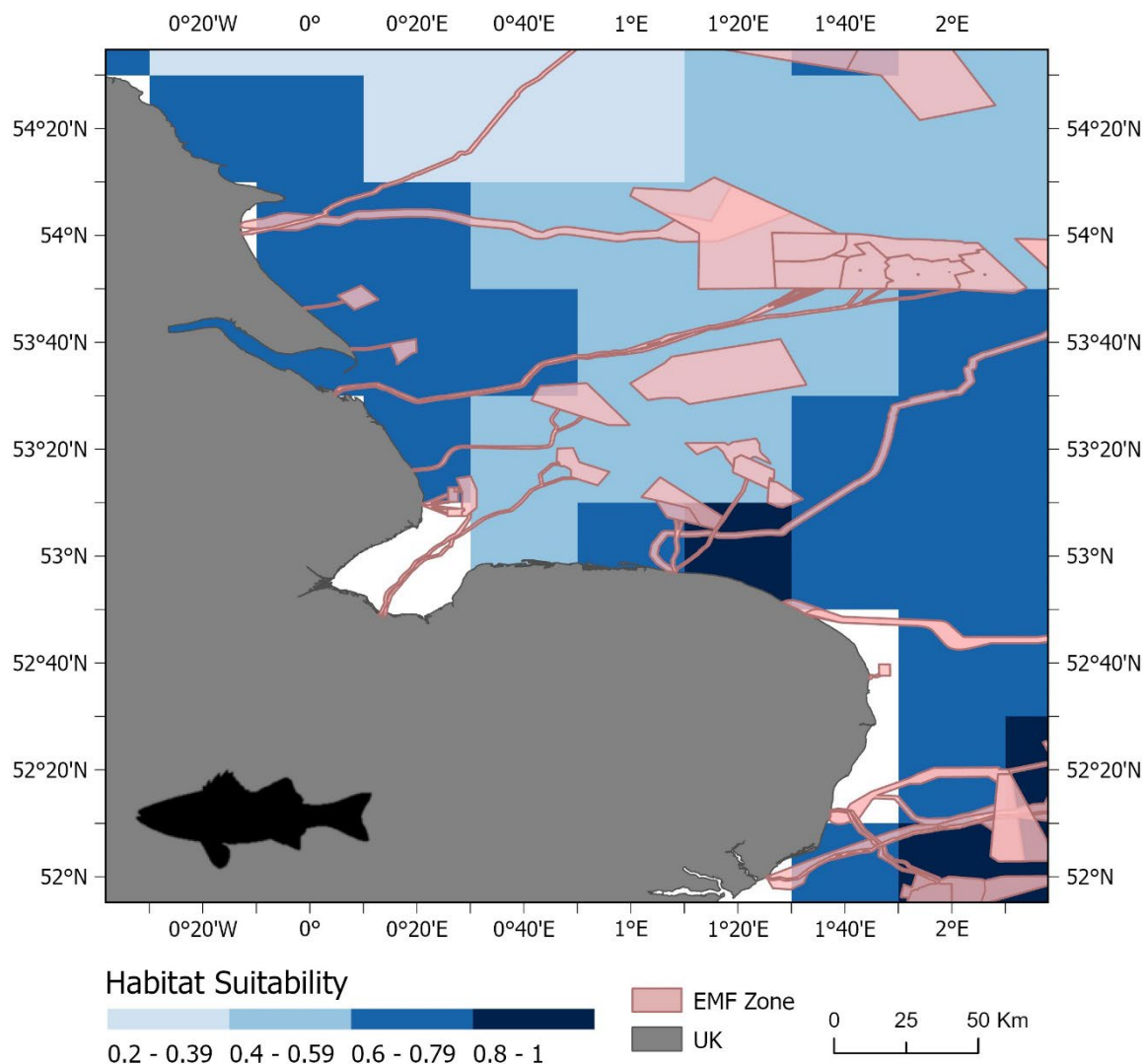


Figure 22. Overlay of European seabass habitat suitability and fixed offshore wind farm footprints (including the export cable route) in Region 1 and part of Region 2. Owing to the coarser scale of the seabass habitat suitability data, the scale was widened to include two adjacent regions where seabass occurred. The darker the blue square, the more suitable the habitat was for the species. The pink areas represent the offshore wind installation footprint with the 50 m EMF zone relating to the extent of the magnetic field in the marine environment associated with the offshore wind infrastructure.

Table 6. The 2D likelihood of encounter for European seabass determined from spatial overlap assessment of species occurrence and EMFs zones. Categories are: a) <25% = low; b) 25-50% = low-medium; c) 50-75% = medium-high; or d) >75% = high. Confidence level is based on the proportion of spatial grid squares with data in relation to the total number of grid squares in the region (i.e. no data; see Likelihood of spatial overlap data table).

A	B	C	D	E	F								G								
					Count of grid cells overlapping EMF zones in region	Weighted proportion of data overlap = (D/C)*B	Count of grid cells overlapping cable EMF zone for each offshore development								Weighted proportion of grid cell overlap with EMF zones for each offshore development = $(F_x / F_{x\text{total}}) * B$						
							i	ii	iii	iv	v	vi	vii	viii	i	ii	iii	iv	v	vi	vii
Blank		3																			
0.01 - 0.19	0.2			0.00											0.00	0.00	0.00	0.00	0.00	0.00	0.00
0.2 - 0.39	0.4	3	2	0.02	2										0.13	0.00	0.00	0.00	0.00	0.00	0.00
0.4 - 0.59	0.6	17	14	0.19	2	3	6		2	1					0.20	0.36	0.45	0.00	0.40	0.30	0.00
0.6 - 0.79	0.8	21	15	0.27	2	2	2	5	1		1	2		2	0.27	0.32	0.20	0.67	0.27	0.00	0.80
0.8 - 1.0	1	4	4	0.09				1		1					0.00	0.00	0.00	0.17	0.00	0.50	0.00
Total		45	35	0.56	6	5	8	6	3	2	1	2		0.60	0.68	0.65	0.83	0.67	0.80	0.80	
	Total # grids cells	48																			
	% data available	93.8																			

Spatial confidence level - Based on grid squares with data and without	
Low	<25%
Low-medium	25-50%
Medium-high	50-75%
High	>75%

4.3.3 Basking shark - migratory species

Basking sharks are found migrating throughout the eastern Irish Sea at certain times of the year with a range of habitat suitability categories across the region (Figure 23). This led to a regional low-medium categorisation of 2D encounter likelihood with a high confidence, based on existing data. (Table 7). However, there was a notable lack of habitat suitability data relating to the nearshore waters, which meant that not all grid overlaps between the coloured grid squares and the EMFs zones of individual OWF infrastructure footprints could be assessed (Figure 23). This is a clear case of where supplementary data should be considered (i.e. the white areas with pink EMF zones off the coast of northern Wales; Figure 23), such as local observer data or coastal surveys conducted for other projects. Where there were overlaps in habitat suitability for the basking shark and each offshore wind development EMF zone, there was a high 2D likelihood of encounter (Table 7). The high categorisation for the individual offshore wind developments 2D likelihood assessment was a result of the developments coinciding with high habitat suitability. Whereas the low-medium regional assessment, related to the variable habitat suitability across the rest of the region. The temporary nature of the basking shark occurrence as it migrates through the area will also reduce the likelihood of encounter with cable EMFs. Further data on the temporal occurrence should be considered if the likelihood of encounter is assessed as medium or high.

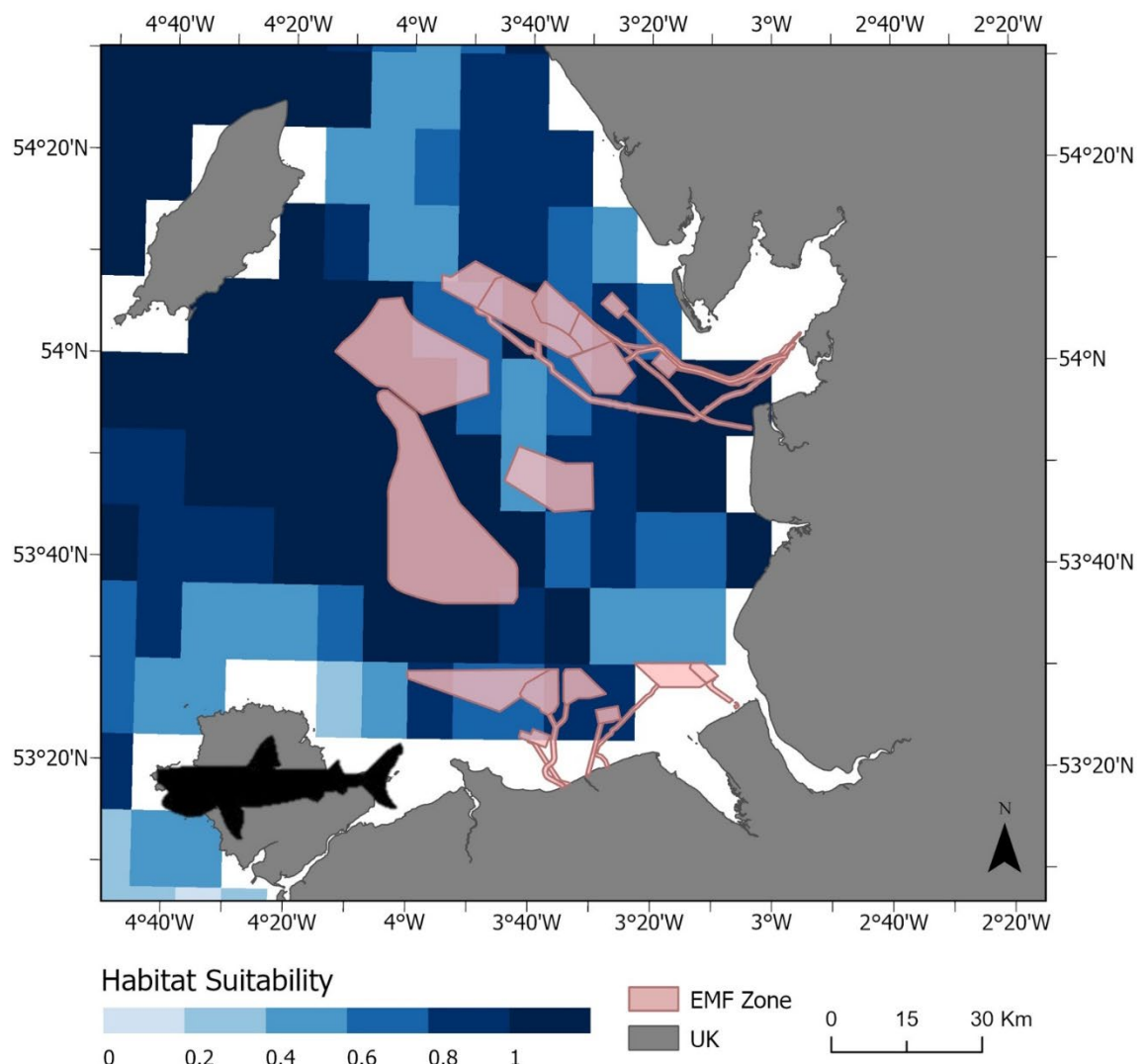


Figure 23. Overlay of Basking shark habitat suitability and fixed offshore wind farm footprints (including the export cable route) in Region 3. The darker the blue data square the more suitable the habitat was for the species. The pink areas represent the offshore wind installation footprint with the 50 m EMF zone relating to the extent of the magnetic field in the marine environment associated with the offshore wind infrastructure.

Table 7. The 2D likelihood of encounter for basking shark determined from spatial overlap assessment of species occurrence and EMFs zones. Categories are: a) <25% = low; b) 25-50% = low-medium; c) 50-75% = medium-high; or d) >75% = high. Confidence level is based on the proportion of spatial grid squares with data in relation to the total number of grid squares in the region (i.e. no data; see Likelihood of spatial overlap data table).

A	B	C	D	E	F				G				
						i	ii	iii	iv	i	ii	iii	iv
Blank		28											
0.01 - 0.19	0.2	0	0	0.00						0.00	0.00	0.00	0.00
0.2 - 0.39	0.4	2	0	0.00						0.00	0.00	0.00	0.00
0.4 - 0.59	0.6	20	2	0.01	1				1	0.05	0.00	0.00	0.30
0.6 - 0.79	0.8	16	8	0.06	4	3				0.29	0.30	0.00	0.00
0.8 - 1.0	1	70	24	0.22	6	5	11	1	1	0.55	0.63	1.00	0.50
Total		108	34	0.29	11	8	11	2	2	0.89	0.93	1.00	0.80
Total # grids cells		136											
% data available		79.4											

Spatial confidence level - Based on grid squares with data and without	
Low	<25%
Low-medium	25-50%
Medium-high	50-75%
High	>75%

4.3.4 Summary

For each of the species' considered, the assessment of the habitat suitability provided a useful approach, which can be consistently applied for different species of interest. When overlaid with the GIS representation of the EMFs zone for offshore wind development footprints within the defined area, it allowed a two-dimensional (2D) assessment and categorisation of encounter likelihood, supported by a level of confidence based on the available spatial data for the species and OSW developments.

The habitat suitability indicated where the species was most likely to occur. The scale of the GIS grid squares is dependent on the scale at which the data were collected and reported. This meant that some of the overlapping assessments were at a coarse scale. This is considered reasonable for the initial evaluation of whether there is any 2D spatial overlap. However, for specific areas where there are several overlapping EMF zones representing different offshore wind developments, then more specific and smaller-scale grid squares may be required for improved local predictions of likelihood of encounter. The advantage of using coarser-scale assessments was that they provided a broader spatial coverage, which was beneficial for an initial cumulative assessment in a region of interest.

It is also important to note that the preceding example assessments relate to adults of the species. As EMFs can affect species at different life stages then relevant life stages should also be assessed. However, it should be acknowledged that most of the data used for habitat suitability assessment come from surveys of adult fish, which are routinely used for fisheries population and stock assessment. Therefore, other data sets should be considered where habitat suitability data of focal receptor species are limited.

4.3.5 Spatial assessment incorporating depth and temporal occurrence

The spatial assessment in the previous section used decadal occurrence data to determine habitat suitability for the selected species. Whilst this provided valuable insight towards understanding the likelihood of encounter between a species and the EMFs associated with subsea power cables, it is constrained to a two-dimensional assessment of spatial overlap. Additionally, the species occurrence data are aggregated over annual periods, and they may not adequately capture many species of interest that have marked seasonal variability, such as migratory elasmobranchs. Therefore, where data allows, a useful extension of the 2D spatial assessment would be to consider the time of year and life history stage when the species may occur within an area (i.e. temporal overlap) and the vertical distribution of the receptor. This would provide a more representative and three-dimensional (3D) assessment between a focal species and the EMF zone, which is particularly important when considering floating offshore wind dynamic cables in the water column.

Depth or vertical distribution data are more limited compared to spatial occurrence and distribution; however, for some species suitable data are routinely collected using acoustic tagging and tracking or via acoustic measurement. A 3D spatial and temporal assessment should therefore be included in the consideration of the likelihood of encounter between species of interest and EMFs from subsea power cables.

4.3.6 General Considerations for Water Depth and Vertical distribution

The likelihood of encounter approach should consider the range of water depths that the receptor inhabits with regard to the extent of the magnetic fields in the surrounding environment. When species are categorised as benthic, pelagic and migratory, there is an implicit assumption that these habitat associations and functional modes predominate. However, as the species of interest occupy a 3D aquatic environment, supporting data for water depth and vertical position/distribution in the water should be provided to justify these assumptions.

Table 8 shows a summary of published evidence on the depth ranges that the three example species (used in the 2D assessment above) inhabit. Depth data over time are usually obtained from depth loggers attached to multiple individuals of the target species (e.g. Newton et al, 2021; Wright et al 2024). However, acoustic methods can provide short-term supplementary data for water depth association where species are distinguishable (Korneliussen et al. 2016). Depth data are referenced against the surface, as the tags use pressure to determine water depth, therefore the depth of the individual fish relative to the seabed is not usually taken into account. This is an evident disadvantage for the current project as the assessment of the fish position and the cable position from the seabed up into the water column is necessary.

Table 8. Summary of vertical and temporal distribution ranges for the three focal species used to estimate spatial overlap with SPC EMFs. The depth ranges represent the most frequent depths that the species inhabit, based on the sources cited. Temporal aspects included represent the seasons in UK waters: Spring (Mar – May); Summer (Jun - Aug); Autumn (Sep – Nov); Winter (Dec - Feb).

Species	Region	Depth Range (m)				Maximum Depth (m)	Sources
		Spring	Summer	Autumn	Winter		
Thornback ray	North Sea	< 20	Data Limited	20 - 35	20 - 35	Data Limited	Hunter <i>et al.</i> 2005
European seabass	North Sea	22 - 39	24 - 26	27 – 31	35 – 41	71	Wright <i>et al.</i> 2024
	English Channel	23 - 39	20 - 21	18 - 28	30 - 37	107	
	Irish Sea	63 - 68	14 - 51	11 - 14	15 - 46	141	
Basking shark	Northeast Atlantic	1 - 1000	1 - 250	1 - 250	1 - 1000	1500	Andrzejaczek <i>et al.</i> 2022; Doherty <i>et al.</i> 2017 and 2019

For the assessment of the 3D likelihood of encounter with SPCs EMFs, the depth ranges of the animals need to be considered relative to where the cable is located (see Figure 25). Within a turbine array of fixed offshore wind developments, power cables exit the monopiles vertically towards the seabed, where they are either laid over the seabed, buried, or covered with hard protection. When buried, export cables usually target a depth of between 1.5 to 3 metres, or in areas of hard substrate they may be buried using HDD several more metres below the seabed level. The magnetic field is not affected by burial, although the depth within the seabed that a cable is buried (or covered) will change the distance between the receptors and the cable surface and the resulting exposure to EMF. Nevertheless, the EMF zone extends into the surrounding environment (both the water and seabed) and therefore,

the likelihood of encounter between the receptor species and the EMF zone will be influenced by the spatial extent of the EMF and the depth range occupied by the receptor species.

Figure 24a, depicts pelagic fish encountering the EMF generated by a buried cable in a shallow nearshore area (depicted by the black broken arrow), whereas in deeper water, the same species will not overlap with the EMF zone (white broken arrow). The range of movement by juvenile pelagic fish is expected to be narrower than adults owing to juveniles associated with the seabed for refuge; this will increase the likelihood of exposure (black broken arrow). The habitat of benthic species (depicted by ray and a crab) may overlap with the EMF zone whilst the cable is operational. This is likely true most of the time; however, some species do move away from the seabed, and potentially away from the EMF zone, as illustrated by the white section of the broken arrow of the shallower ray in Figure 24. When considering floating offshore wind dynamic cables, the relationship between the depth range of the species and where the cable is in the water column should be assessed (Figure 24b). The same approach is applicable as for the fixed cable scenario. The life stage, habitat association and location should also be considered for all species. Some pelagic species use shallow and/or seabed habitats for spawning or juvenile nursery areas. Therefore, whilst the adults may not encounter the EMF zone, other life stages may encounter them. For species that have planktonic life stages, such as the crustaceans, vertical migration may lead to encounter with the EMF zone (Figure 24b). Data on early life stage habitat use are often limited. However, it is appropriate to include the early life stage when assessing the likelihood of encountering SPC EMFs.

Some species, such as Basking sharks, may also enter deeper waters (Table 9). Consequently, the frequency and duration of these excursions should be considered, and the likelihood of EMF encounter reassessed, if necessary, and where data allow. The timing of movements of the receptor, such as migration, is another important aspect to consider. Therefore, to appropriately assess the likelihood of encounter by a migratory receptor, the EMF zone should reflect the power generation levels during the key migration period, which may be lower than those observed during the windier winter months.

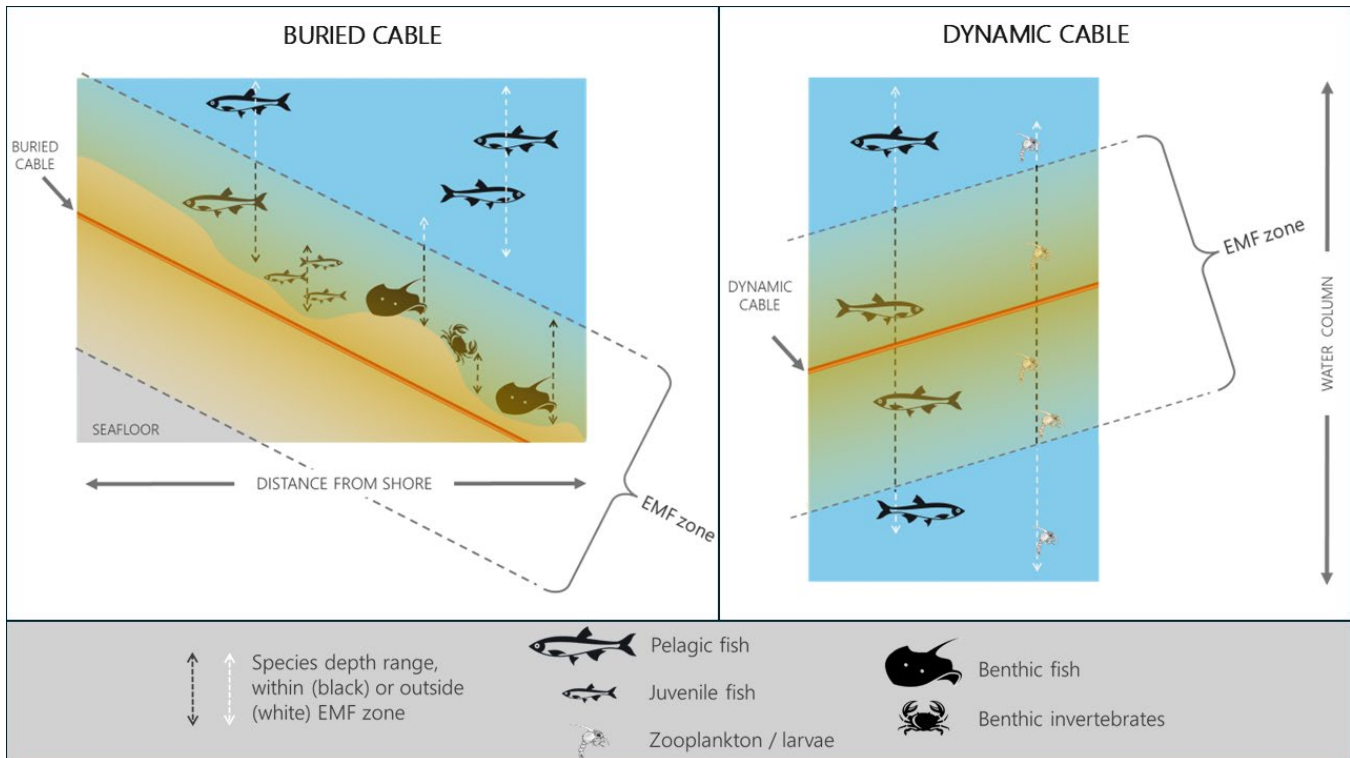


Figure 24. Depiction of the relationship between target species depth ranges (dotted arrows) and the location of the subsea power cable EMF zones for buried cables from fixed offshore wind (left) and dynamic cables from floating offshore wind (right). The vertical position and habitat range in the water column of different receptors and life stages will determine how likely they will encounter the EMFs generated by the power cable. Image credits: pelagic, juvenile fish and benthic invertebrate icons from Vecteezy, benthic fish icon from Noun Project.

5. Framework to estimate the likelihood of species encounter (Objective 4)

The fourth objective of the FLOWERS WP2 was the development of a framework to determine the likelihood of encounter between EM-receptive species and dynamic cable EMF. As highlighted earlier, we used fixed cable scenarios from offshore wind developments to provide the necessary evidence to develop the approach. Figure 26 shows how the outputs from Objectives 1, 2 and 3 (as described in the previous sections of the report) need to be drawn together to meet Objective 4.

The cable(s) layout and configuration, and power transmission characteristics must be specified and then used in models to estimate the magnetic field extent (Objective 1). Where data are available the model should be validated, which could use a comparison between the magnetic field modelling and the measurements of fixed SPC sites (Objective 2). These data are then used to define the EMF zone around the spatial footprint of the offshore wind subsea power cabling (existing and planned), which coincides with the distribution of the focal receptor (Objective 3). Drawing these elements together provides an initial assessment of the likelihood of spatial overlap of species and cable EMFs within an area of interest, summarised in Figure 25.

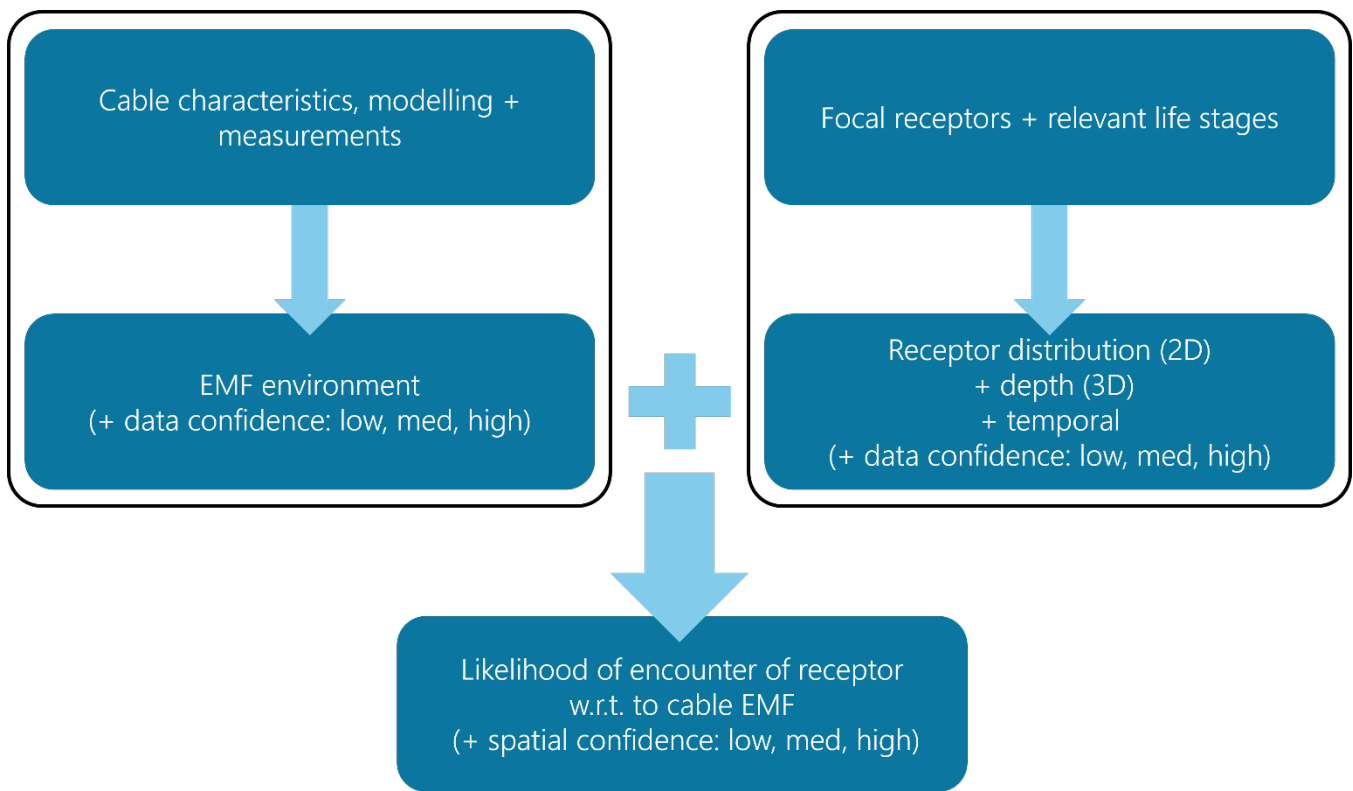


Figure 25. The essential elements identified through the FLOWERS project to determine the likelihood of encounter between focal species and subsea power cable EMFs. These elements are demonstrated in prior sections of the report through Objectives 1, 2, and 3.

Following the 2D likelihood of encounter assessment, it is possible to identify, geographically, where there is overlap between the EMF zones and the receptor of interest (e.g. Figure 21, based on habitat suitability). In areas with greater habitat suitability, there is an expectation of a higher likelihood of encounter with EMF for the receptor. Where there is reliance on the 2D assessment, the assumption is that the focal receptor is present in that area and does not take into account the vertical distribution of the receptor (whether benthic, demersal or pelagic; Table 9) or the temporal nature of the receptor occurrence (e.g. seasonality). Therefore, it is important to build on the 2D assessment and integrate vertical distribution data to provide a 3D assessment and subsequently consider the temporal nature of the receptors occurrence in the study area. In each stage of data integration, where data are lacking or unreliable, this will lower the confidence of the assessment. If overlap is apparent between the species (regardless of life stage) and the EMF zone, but the data are insufficient for a robust assessment, this would require further data integration where available and possibly additional data collection (e.g. receptor distribution in near shore areas; EMF measurements) and or modelling (e.g. receptor migration routes, EMF modelling). This may require expert consultation and advice. Where additional data are collected, the assessment would be revisited to improve the confidence in the outcome. Another key consideration at the start of the assessment is the life history stage and habitat dependency (e.g. differences between benthic spawning and pelagic spawning; juvenile dispersal within the water column versus use of shallow-water benthic refuges) and this may require different data use for each life stage that may encounter the EMF zone.

By defining the EMF environment and identifying the local occurrence of three focal species, the likelihood of encounter between the species and the EMF zone associated with fixed cables, was determined. The applicability of this stepwise approach was demonstrated using three geographic regions and a range of model receptors. This is presented as a framework that can be easily applied to an offshore energy EMF environment and receptor of interest.

5.1 Stepwise framework to determine the likelihood of EMF encounter for target species – applied to Floating Offshore Wind Developments

Here a structured framework that reflects an effective scoping assessment to define the likelihood of encounter for a receptor in an EMF zone, incorporating consideration of depth and temporal variability, is set out (Figure 26). The framework is considered to be version 1 with the expectation that it can be enhanced as knowledge on the topic area advances.

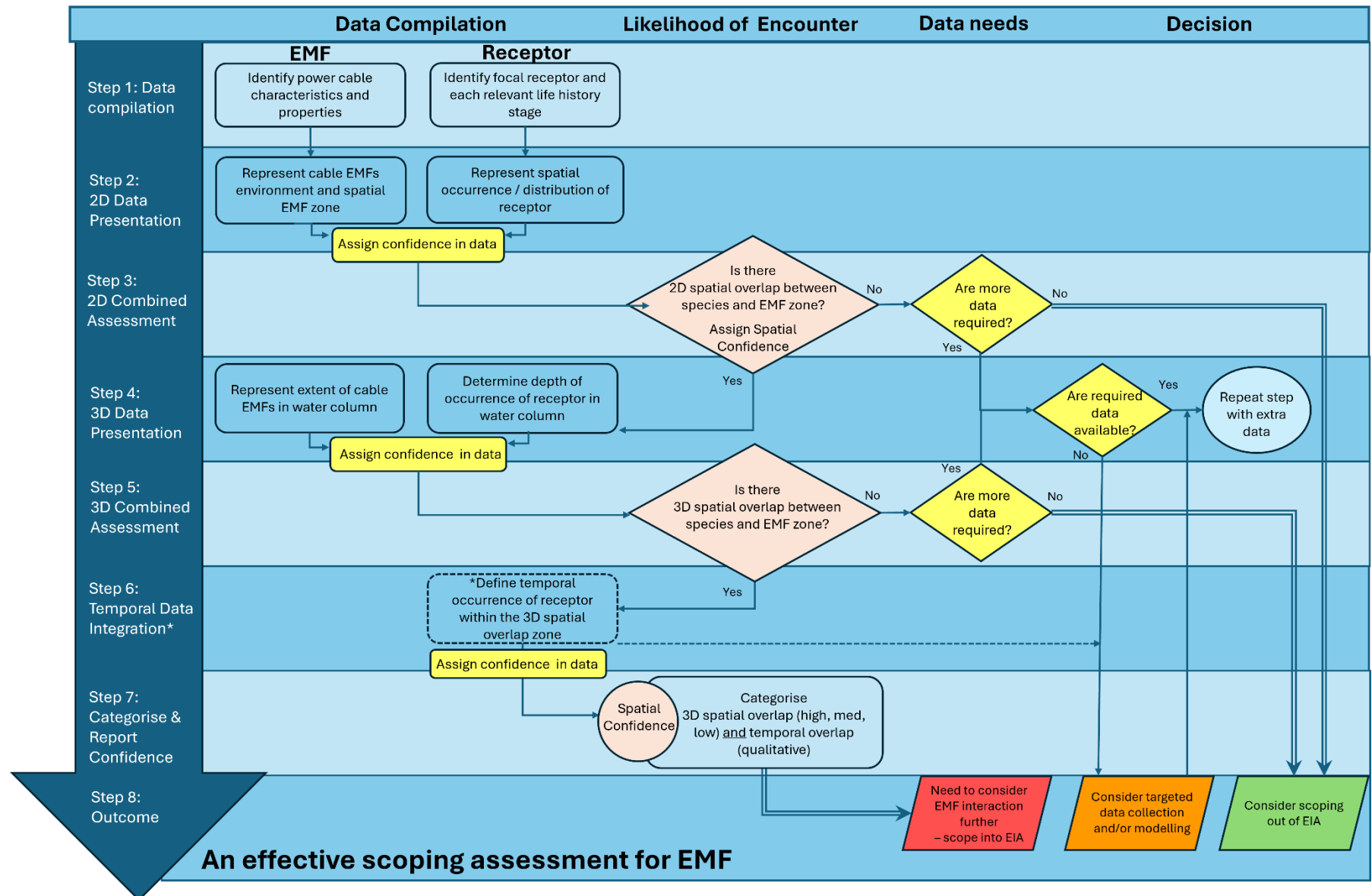


Figure 26. The stepwise framework for determining the likelihood of encounter between a focal receptor and EMFs associated with subsea power cable areas. The eight step framework should be used for each species and life history stage of interest. The framework presents an iterative approach to data compilation and presentation (including assignment of data confidence), a combined spatial assessment in 2D and subsequently 3D, with consideration of temporal occurrence of the receptor taxa. The return loop ensures that, where further spatial or ecological data are required, they can be sourced and integrated before a suitable assessment of the likelihood of encounter can be made. This framework is an effective scoping assessment of EMF enabling a justified decision to scope into or out of the Environmental Impact Assessment process.

The framework set out in Figure 1 has the following eight steps to follow:

Step 1: Data Compilation

- Determine floating cable characteristics and properties.
- Identify focal receptor and each relevant life-history stage.

Step 2: Two-dimensional Data Presentation

- Represent the cable EMFs environment and spatial EMF zone.
- Represent spatial occurrence/distribution of receptor.
- Assign the confidence in the data for both EMF and the receptor (refer to Table 5) and consider improvements where possible.

Step 3: Two-dimensional Combined Assessment

- Combine the outputs of Steps 1 and 2 to determine if there is spatial overlap between the species and the EMF zone and assign the spatial confidence (i.e. confidence in the 2D spatial assessment).
 - If there is an overlap, go to Step 4.
 - If no overlap, consider if there are sufficient data.
 - If more data are required, check the availability of the data and either repeat the step with additional data (i.e. go back to step 2), or consider additional data collection and/or modelling and then repeat the step (i.e. go back to step 2).
 - If no more data are required, the outcome is to consider scoping out of the EIA and the process of considering the likelihood of EMF encounter can stop.

Step 4: Three-dimensional Data Presentation

- Represent the extent of cable EMFs in the water column (based on Step 2).
- Determine the depth/vertical occurrence of the species/receptor in the water column.
- Assign the confidence in the data for both EMF and the receptor taxa in the water column (refer to Table 5) and consider improvements where possible.

Step 5: Three-dimensional Combined Assessment

- Combine the outputs of Steps 3 and 4 to determine if there is 3D spatial overlap between the species and the EMF zone and assign the spatial confidence (i.e. confidence in the 3D spatial assessment).
 - If there is an overlap, go to Step 6.
 - If no overlap, consider if there are sufficient data.
 - If more data are required, check the availability of the data and either repeat the step with additional data (i.e. go back to step 4), or, consider additional data collection and/or modelling and then repeat the step (i.e. go back to step 4).
 - If no more data are required, the outcome is to consider scoping out of the EIA (Step 8) and the process of considering the likelihood of EMF encounter can stop.

Step 6: Temporal Data Integration

- Define temporal occurrence of receptor within the three-dimensional spatial overlap zone and assign confidence in data (refer to Table 5).

Step 7: Categorise and Report Confidence

- Categorise three-dimensional spatial overlap (high, medium, low) and report spatial confidence together with data confidence (per EMF data, receptor data and temporal data).
- Reaching Step 7 indicates a likelihood of encounter for the receptor; therefore, the outcome is that EMF should be scoped into the impact prediction process during the formal EIA.
- *Note:* The compilation tables (Table 3 and Table 4) used for the combined assessment of spatial overlap (Steps 3 and 5) provide some evidence which could be used in the impact prediction assessment of the EIA.

Step 8: Outcome

- There are three possible outcomes from the framework.
 1. Need to consider EMF interaction further – scope into EIA.
 2. Consider targeted data collection and/or modelling
 3. Consider scoping out of EIA.

Table 9. The confidence categories and the associated criteria for the 2D, 3D and temporal data separated into EMF and Receptor criteria.

Data type	Confidence Category	EMF criteria	Receptor criteria
2D	Low	Cable EMF model based on maximum power; no power variation included; no validation of model with measurements	Spatial presence/absence data with areas of missing data; data only available for 1-3 years
	Medium	Cable EMF model based on maximum power with validation OR power variation included in model but no validation of model with measurements	Spatial data with some distribution or abundance indication; OR proxy such as Habitat Suitability metric; data available for 3+ years
	High	Cable EMF model based on representative power variation with validation through measurements	Spatial data with distribution or abundance or density quantified; OR proxy such as Habitat Suitability metric with evidence of high metric confidence; data covering 3+ years
3D	Low		Approximate depth range
	Medium		Depth range supported by water column vertical distribution data
	High		Quantified water column vertical distribution data
Temporal	Low		No temporal consideration
	Medium		Seasonal consideration based on data or proxy
	High		Temporal occurrence for defined time periods (e.g. months) determined from primary data

To illustrate the application of the stepwise framework, each of the steps are followed for the Celtic Sea Round 5 floating offshore wind example using the adult basking shark as the receptor (Figure), detailed in Section 6. This provides the guidance on applying the framework for a user.

6. Guidance to apply the framework (objective 5)

6.1 Setting the scoping assessment framework in context

The EIA process for offshore wind farms in the UK is designed to assess the significance of a range of potential environmental impacts of proposed developments. In general, it includes the following steps:

1. **Screening:** Determining whether a project require an EIA.
2. **Scoping:** Identifying the key environmental issues to be addressed.
3. **Impact Assessment:** Evaluating the potential impacts on the environment, including cumulative and inter-related effects.
4. **Mitigation:** Proposing measures to prevent, reduce, or offset significant adverse effects.
5. **Monitoring:** Assessing the actual impacts post-consent and ensuring compliance with the predicted assessments

Current consideration of potential impacts of EMFs on receptors, within the EIA process occurs during the Scoping stage, relies on existing information from the literature to decide whether EMFs should be scoped in or out.

Historically, EMFs were scoped out of the EIA process. The advice regarding cables, was from the UK EN-3 National Policy Statement (DECC, 2011) stipulating that EIAs should assess the physical effects of cable installation. This meant that considerations of physical effects on cables, should consider effects on receptors including fish, seabed habitats, marine mammals and birds, spawning, nursery and feeding grounds, and over-wintering areas and migration routes of species of concern. Explicit advice on EMF effects was that the residual impact would be negligible following burial; therefore, EMF could be discounted. This advice is now regarded as out-of-date, as the science has moved on and several publications now highlight the need to consider EMF impacts on receptors (Hutchison *et al.*, 2021; Klimley *et al.*, 2021; Hermans *et al.*, 2023).

A recent report (Hutchison and Gill, 2025) established a common understanding of current knowledge regarding the topic of EMF with a focus on strategically improving the evidence base where needed. To improve the evidence base there is a need to better define the emissions EMFs from subsea cables, to determine the true encounter rate of EMFs for aquatic species and more clearly define responses to cable EMFs. An understanding of appropriate mitigations may be beneficial; however, this will only be required if a population level impact is determined through appropriate evidence.

These topics are now better represented in the 2023 updated EN-3 National Policy Statement (EN-3 NPS; DESNZ, 2023), which includes assessment of EMFs owing to potential impacts on fish, shellfish, subtidal habitats and species. EN-3 NPS is applicable to certain offshore wind farm projects in England and Wales. In Scotland, the regulator is recommended to take this report into consideration when providing advice to applicants on EIA scoping, during application determination and, if required, when setting any EMF specific requirements for mitigation and monitoring.

The updated EN-3 NPS now more accurately states that burial (including external cable protection) will increase the distance between the maximum EMF intensity and animals, which better reflects the real-life environmental conditions on which to base an impact assessment. It also advised that EMFs should be monitored to provide evidence to inform future EIAs (owing to the uncertainty of cumulative impacts from multiple cables and those with larger power transmission). For floating offshore wind, the EN-3 NPS states that alternative monitoring and mitigation consideration may be required.

Here application of the likelihood of encounter assessment framework (Section 5), is presented as an effective scoping exercise to provide a justified decision for the inclusion or exclusions of a receptor in the impact prediction

process. The application is illustrated for the Celtic Sea Round 5 selecting the adult basking shark as the focal receptor.

6.1.1 Step 1. Data compilation

To complete Step 1, data is compiled to determine the floating offshore wind farm cable characteristics and properties, together with data on the focal receptor for each life-history stage of relevance.

Determine floating cable characteristics and properties

For the cable data, this includes the information on the type of cabling (HVAC or HVDC) to be used, for both the interarray cabling and the export cable(s). The number of cables, the cable characteristics, and the relationship between the cable materials and their configuration also need to be known, along with the maximum power rating of the cable, as well as the electrical current transmitted. These data will need to reflect the range of currents transmitted during a typical year, based on wind resource and cable power predictions (Note: if available, representative data from existing and comparable offshore wind cables could be used). Once these data have been obtained, the magnetic field can be estimated using the best available modelling at the time. In this scenario, the data available was limited to the floating offshore wind development area, as cable routes were not yet defined.

Identify the focal receptor and data for each relevant life stage

The adult basking shark was identified as a focal species that had potential to encounter EMFs and should be taken through the scoping assessment. The reasoning for the decision is captured in Section 4.1, Table 2, summarised below for ease.

Table 10. The focal receptor and their attributes, selected for spatial occurrence and distribution analysis within EMF fieldwork region of interest. This information is repeated from Table 2, for ease of the reader.

Category	Selection Criteria			Species
Migratory – large scale	Taxonomic group Ecology Life stage Status EM-sense	Elasmobranch Epipelagic and Migratory – regional scale Adult Conservation importance Electromagnetic sense (induction)		Basking shark (<i>Cetorhinus maximus</i>)

Data collation relevant to the basking sharks was reported in Section 4.1, and Table 9, summarised here for ease;

- Distribution records (2005-2014), based on multiple habitat suitability models (Couce *et al.*, 2025; Townhill *et al.*, 2023).
- Data from the Global Biodiversity Information Facility (GBIF, 2021)
- Data from the Basking Shark Watch Database 1987-2020 (Austin *et al.*, 2019).

The species distribution models used the Intergovernmental Panel on Climate Change (IPCC) ‘Representative Concentration Pathways’ (RCPs) climate projections for each decade to 2100 for basking shark (Couce *et al.*, 2025). Here the training data for the decade 2020 to represent the species’ current habitat suitability in UK waters was used. (see Section 4.1 for full details).

6.1.2 Step 2. Two-dimensional Data Presentation

Define the cable EMFs zone

At the time of the scoping assessment, there were no details on the cable array or export cables; therefore, no cable routes are incorporated in the map. However, they should be added, when available, to allow a more representative estimation of the EMF zone. Using the best available information at the time of the assessment, the 2D data presentation focused on the planning areas, applying the same EMF zone to all, based on comparable measurements undertaken at the fixed cables sites, reported in Section 3. In the fixed cable cases studied, it was noted that there was often more than one export cable. Therefore, the number of cables within the turbine array and exporting to shore should be included for the floating offshore wind scenario as well. The planning areas and EMF zones were uploaded to GIS (not shown).

Represent the spatial occurrence of receptor

Distribution data compiled in step 1, were projected onto a $0.25^\circ \times 0.25^\circ$ study grid in GIS (not shown), and cells with data were first classed as “presence” sites, while remaining cells were classed as “absence” sites. The presence grid squares were then assigned a habitat suitability category between 0 and 1.0 using equal intervals for the categories. While this example used the habitat suitability approach described in Section 4.1, it is noteworthy that an equivalent data set showing the spatial distribution of the focal receptor *density* could be used where available.

Assign Data Confidence

The spatial occurrence of the basking shark in the eastern Celtic Sea was determined and is shown in **Figure 27** overlaid with the EMF zone for the offshore wind planning areas and known cable routes.

The Data Confidence was assigned based on the metrics outlined in Table 5. Explanations are provided below.

- **EMF Data Confidence: Low.** The specific cable routes were not available, nor the specific cable characteristics, therefore the EMF zone was based on a fixed cable proxy and applied to the floating OSW planning areas. Data confidence can be improved where the scoping assessment is revisited in future.
- **Receptor Data Confidence: Medium.** Data for the occurrence of basking sharks was based on multiple Habitat Suitability models (a proxy) supplemented with multiple sources of occurrence data, and data were collated from multiple years.
- **Improvements:** Any available steps to improve the data confidence should be considered prior to moving to the next step. No improvements are available at this time.

6.1.3 Step 3. Two-dimensional Combined Assessment

The two sets of spatial data were then overlaid within the GIS to determine the likelihood of encounter in 2D. As shown in Figure 27, there is spatial overlap between basking shark occurrence and the EMF zones for the planning areas.

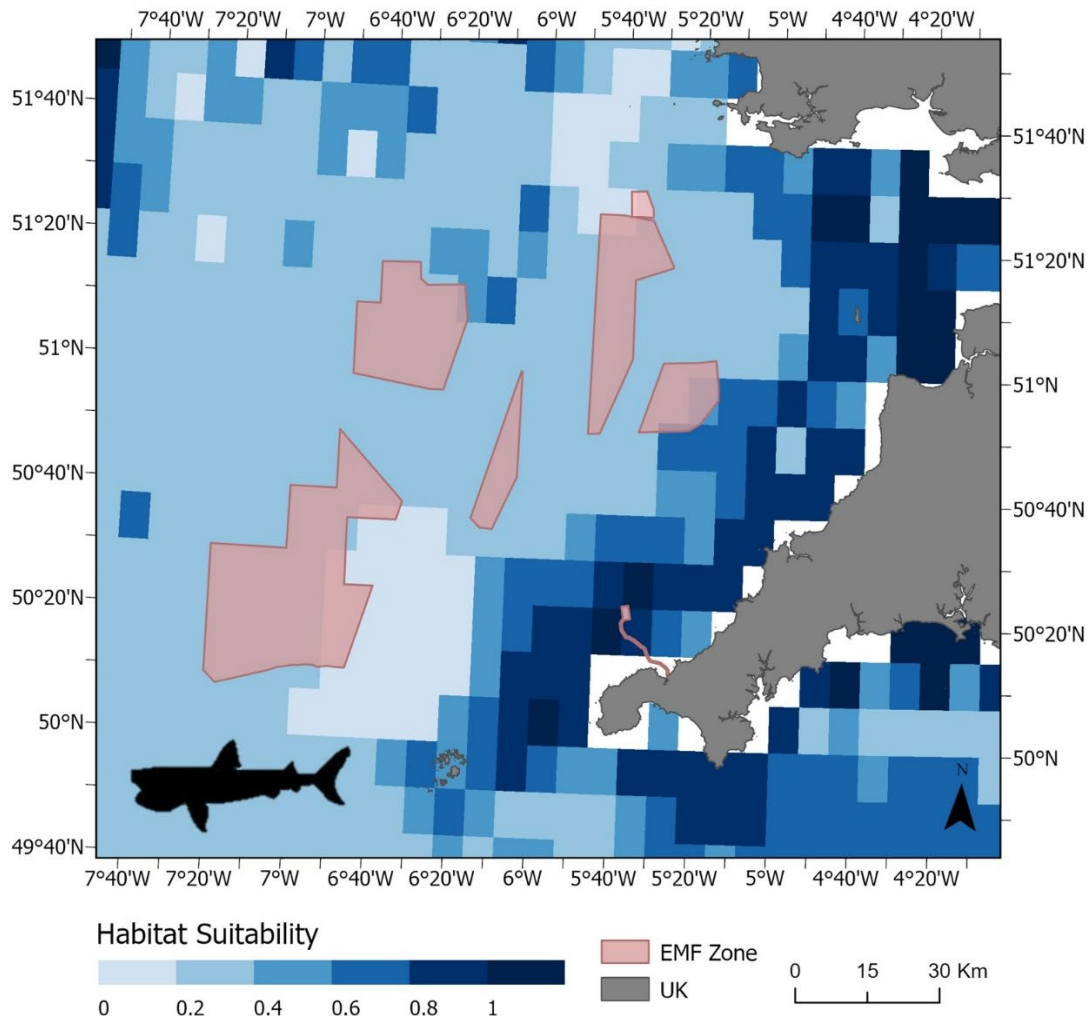


Figure 27. The two-dimensional data presentation for basking sharks and EMF zones associated with floating offshore wind in the Celtic Sea. The eastern Celtic Sea habitat suitability for basking sharks is presented from multiple data sources with a medium data confidence. The Round 5 offshore wind planning area is included, represented with the pink-coloured EMF zone applied. Note: The planning area assumes that floating offshore wind will occur across the extent shown. However, the export cable routes are not included due to unavailability at the time of the scoping assessment.

The steps outlined in Section 4.2 were followed and results added to the table template (Table 4) with the results from shown in Table . The habitat suitability was displayed as grid box categories in column A. Referring to Table 3, the weighting was applied in column B, per grid box category (Table 4). The total count of boxes per grid box category was calculated for the total region (Column C; including grid boxes with no data), and for those that overlap with the EMF zone (Column D). The weighted proportion of overlap was then calculated (Column E) to avoid inflating the result based on the extent of the region mapped. These steps were then repeated per development area (Column F and G).

Assign Spatial Confidence:

- **Spatial Confidence based on region: *High*.** With reference to Table 11 (green table), the spatial confidence was assigned as high because the data coverage for the basking shark occurrence across the region was 96.1%. This is based on the region as a whole and that there were only a few white areas indicating 'no data'.

Table 11. Likelihood of encounter for basking shark determined from 2D spatial overlap assessment of species occurrence and EMFs zones of floating offshore wind developments in the Celtic Sea.

A	B	C	D	E	F					G					
						i	ii	iii	iv	v	i	ii	iii	iv	v
Blank		19													
0.01- 0.19	0.2	36	10	0.00	8				2	0	0.06	0.00	0.00	0.06	0.00
0.2 - 0.39	0.4	258	51	0.04	19	15	6	13	5	0.28	0.38	0.40	0.74	0.29	
0.4 – 0.59	0.6	51	2	0.00		1			1	0.00	0.04	0.00	0.00	0.09	
0.6 – 0.79	0.8	55	2	0.00					1	0.00	0.00	0.00	0.00	0.11	
0.8 – 1.0	1	68	4	0.01						0.00	0.00	0.00	0.00	0.00	
Total		468	69	0.06	27	16	6	15	7	0.34	0.41	0.40	0.80	0.49	
	Total # grids cells	487													
	% data available	96.1													

Spatial confidence level - Based on grid squares with data and without	
Low	<25%
Low-medium	25-50%
Medium-high	50-75%
High	>75%

Total region

Figure 27 shows an overlap in the occurrence of basking sharks and EMF zones. The spatial confidence was 96.1% and therefore categorised as high Table 11. However, the suitable habitat is categorised as low to medium for most of the planning areas (light blue squares, 0.2-0.4), and the estimation of the overall weighted proportion of overlap was very low at 0.06 (Table 11, column E total). This low categorisation for the weighted proportion of overlap, despite the high spatial confidence level, was due to the extensive spatial data coverage for the region (96.1%) but lower incidence of occurrence in the development EMF zones.

Individual developments

It is important to note that part of the reason for this low proportion of overlap is that the region defined covers a large part of the eastern Celtic Sea, while the offshore planning areas are a small part of this region. For this reason, the weighted proportion of overlap for each development area is more representative of the likelihood of encounter, where it ranged from 0.34 with one at 0.80 (Table 11, column G totals). Referring to Table 3 for the categorisation, if each individual planning area is considered, then the weighted proportions indicate that most have a low-medium likelihood of encounter categorisation, with one development being categorised as high.

While the assessment indicates overlap of the receptor and EMF zone and therefore this means moving to step 4, it is also worthy of note that this step is completed with some very clear data deficiencies in the EMF zone (as detailed in step 2). Therefore, the recommendation is that this stage is revisited when better data become available. In particular, the habitat areas potentially more favourable to adult basking sharks are nearer the coast and that the cable export routes are not included in the current assessment lowering the confidence in this assessment (Figure 26, Table 11). As there was some spatial overlap categorised as medium or high, the assessment continues to Step 4.

6.1.4 Step 4. Three-dimensional Data Presentation

Understanding the potential for overlap in basking shark vertical location in relation to the EMF extent of dynamic cables requires knowledge on the depth of deployment of the cable(s), the variability in this depth and the depths inhabited by the basking sharks. Dynamic cables, as their name suggests, move in the water column, and so will the EMF zone, as will the basking sharks.

Represent the extent of EMF in the water column.

This step is crucial when estimating the EMF zone for floating offshore wind, as the dynamic cable will create the opportunity for receptors to be exposed to the magnetic field above, around and below the cable. Therefore, the volume of the water column where the EMF will be present is greater than in the fixed, seabed laid or buried cable scenario if the cable properties were comparable (shown in Figure 24).

At present, an estimation of the range of depths of cable(s) deployed in the water column should be determined from consultation with the cable engineers, and this should be available from the cable data compilation (Steps 1 and 2). While the 3D consideration is an additional step, the data compiled in step 1 and used in step 2 to define the EMF spatial extent (through a model and/or through measurement data) is applicable here since the emission occurs around the cable. There may be no need to do additional modelling, rather, consider the outputs of step 2 in the third dimension. However, modelling of dynamic cables and potential influence of flex on the EMF is not well understood, and as that research area develops, this could be enhanced. Here, as for the 2D combined assessment, the proxy EMF zone was applied but in the vertical dimension.

Determine the depth/vertical occurrence of the species/receptor in the water column

For basking sharks, the known depth distribution indicates they are typically found in depths of 1-1000 m, with a maximum known range of 1500 m (Table 12). These data, compared with the EMF in the vertical water column data, will determine whether they will encounter the EMF generated by the dynamic cable(s) in Step 5.

Table 12. Summary of vertical distribution ranges for the basking shark. The depth ranges represent the most frequent depths inhabited, based on literature sources cited. Variation in vertical distribution are included, for UK waters: Spring (Mar – May); Summer (Jun - Aug); Autumn (Sep – Nov); Winter (Dec - Feb). This information is repeated from Table 1, for ease of the reader.

Species	Region	Depth Range (m)				Maximum Depth (m)	Sources
		Spring	Summer	Autumn	Winter		
Basking shark	Northeast Atlantic	1 - 1000	1 - 250	1 - 250	1 - 1000	1500	Andrzejaczek <i>et al.</i> 2022; Doherty <i>et al.</i> 2017 and 2019

Assign Data Confidence

The Data Confidence was assigned based on the metrics outlined in Table 5 as follows:

- **EMF Data Confidence: Low.** Justification is the same as for the 2D EMF data confidence.
- **Receptor Data Confidence: Medium.** Data for the vertical occurrence of basking sharks was based on multiple sources of vertical occurrence data from literature.
- **Improvements:** Any available steps to improve the data confidence should be considered prior to moving to the next step. No improvements were available at this time.

6.1.5 Step 5. Three-dimensional Combined Assessment

Combining the data from the steps leading to the 2D combined assessment with information on the depth of occurrence, a 3D combined assessment is possible, providing a more robust assessment of the likelihood of encounter for the basking sharks and the floating offshore wind development areas. Since basking sharks swim near the surface and at a range of depths (Table 12), the vertical occurrence of the basking shark overlaps with the proxy EMF zone, revealing a 3-dimensional overlap.

6.1.6 Step 6. Temporal Data Integration

The last step draws together the evidence of spatial and depth overlap, with temporal data if available. These data indicate the amount of time that the receptor will be in the area and are an important component of the likelihood of encounter assessment.

For basking sharks, the habitat suitability data suggest they are present for most of the year and the vertical occurrence sources indicate seasonality in their depth (Table 12). However, as basking sharks are known to be migratory, knowledge on their temporal occurrence should be included to improve confidence in the assessment. Table 9 indicates that basking sharks are more frequently found in shallower water through Spring and Summer. This is particularly important as migration routes may take them into shallower waters or across areas where export cables are routed at certain times of the year.

Assign Data Confidence

The Data Confidence was assigned based on the metrics outlined in Table 5 as follows:

- **Temporal Data Confidence: Medium.** Data for the temporal occurrence of basking sharks was based on seasonal data from two sources (*Table*).
- **Improvements:** Any available steps to improve the data confidence should be considered prior to moving to the next step. No improvements are available at this time.

6.1.7 Step 7 Categorise and Report Confidence

The prior steps, making use of 2D and 3D spatial data and temporal data (where available), lead to a categorisation of the Likelihood of Encounter. Here, referring to Table 4, the qualitative three-category (low, medium, or high) likelihood of encounter rating is defined, and reported with the multiple data confidence metrics and the spatial confidence (Table). It is important to understand this is a proposed starting point for an effective scoping assessment. As further data and evidence become available the assessment can be revisited and developed further.

Table 13 13. Summary of the likelihood of encounter for basking sharks, determined from spatial overlap assessment of habitat suitability and EMFs zones associated with floating offshore wind developments. The likelihood of encounter for the region and individual developments is summarised in (a) and the confidence metrics for each data set with the spatial confidence for the region is detailed in (b). Likelihood of encounter categories are: a) <25% = low; b) 25-50% = low-medium; c) 50-75% = medium-high; or d) >75% = high. Spatial confidence level is based on the proportion of spatial grid squares with data in relation to the total number of grid squares in the region (i.e. no data; see Likelihood of spatial overlap data table). For assessment data see Table, in Step 3. .

(a) Likelihood of Encounter						
	Defined region	Individual offshore wind developments*				
		i	ii	iii	iv	v
Likelihood of 2D spatial overlap for species (blue boxes)	0.06	0.34	0.41	0.40	0.80	0.49
Likelihood of species encounter with EMF zones	Low	Low-medium	Low-medium	Low-medium	High	Low-medium
Vertical Encounter	Yes	Yes	Yes	Yes	Yes	Yes
Temporal Encounter	Seasonal	Seasonal	Seasonal	Seasonal	Seasonal	Seasonal

(b) Confidence metrics				
Data Confidence				Spatial Confidence for Region
EMF	Receptor	Vertical	Temporal	
Low	Medium	Medium	Medium	High

* prior to cable routes being known

6.1.8 Step 8. Outcome

There are three outcomes possible within this framework; to scope in, collect more data and/or model or to scope out (Figure 27). The application of the scoping framework suggests that for basking sharks in Round 5 areas of the Celtic Sea, the EIA scoping stage should consider EMFs for the focal receptor in the EIA process (see Section 6). The data gathering undertaken during the EMF likelihood of encounter assessment will provide some evidence that can be used at the within the EIA process. However, the EIA prediction stage will then require more specific evidence gathering and consideration of the scale of predicted impact. The likelihood of encounter assessment can be integrated into the evidence base used in the EIA process and built upon with evidence of effects and analyses of potential impacts.

The scoping framework is designed to be revisited and updated as new information becomes available, such as cable routes, magnetic field, electrical field or movement data for a receptor. Improved evidence will also enhance the confidence categorisation. This can then lead to recommendations for determining the risk of potential impact with an associated uncertainty categorisation based on available knowledge. Thereby, supporting the assessment of the potential impact of EMFs based on geographic location and cable properties.

A note on the return loops - Are more data required?

In step 3 and Step 5 for the 2D and 3D combined assessments, respectively, where the answer is no overlap, there is a return loop (Figure). The return loop requires that the outcome of the combined assessment is critiqued to determine if the outcome of 'no overlap' is robust enough to be accepted or, if there is a requirement for more data. Following this reconsideration for data improvement, if the data are available, the prior step is repeated with the additional data. If no data are available to be integrated, the outcome is to consider targeted data collection and/or modelling for either the EMF or the receptor where there would be an improved assessment.

For the basking shark and floating offshore wind example here, as detailed in Steps 2 and 4, the confidence in the EMF data is low due to the knowledge on dynamic cables routes and cable characteristics in the Round 5 area being unavailable, but no additional data were available at the time of the assessment and no additional data collection could be undertaken. The overlap indicated by the 2D and 3D assessment was sufficient to justify scoping the basking shark and EMF into the impact prediction process within the EIA. However, these data gaps should be addressed to improve the assessment. When further data become available, for example, later in the development process, through research into dynamic cable EMFs or through post-consent monitoring, the new data sources should be integrated and the assessment repeated to improve the knowledge base.

6.1.9 Moving forward in predicting impacts

A recent report (Hutchison and Gill, 2025) established a common understanding of current knowledge regarding the topic of EMF with a focus on strategically improving the evidence base where needed. A main goal of the report was to improve the understanding of the current evidence base for use in the environmental impact assessments, for developers, regulators and advisors. Through better and consistent understanding of the key elements for EMF and the evidence base, more robust decision making will result to support the sustainable development of offshore wind towards delivering green energy targets. The primary outcome of interest when assessing the potential impacts of EMFs is the determination of the biological significance of the impact, which will be manifest at the population level. To address this potential impacts effectively, the evidence required is in relation to the EMF emissions, the encounter rate between the receptor and the EMFs, and the responses of receptors to the EMFs (Figure 28). Where a population level impact is determined a mitigation may be required.

The evidence base could be improved by building on the framework to determine the likelihood of encounter, to establish a more robust assessment to define the EMF encounter rate for the focal receptor. This evidence would result from a finer resolution of data being compiled and could subsequently be combined with evidence of effects to predict potential impacts.

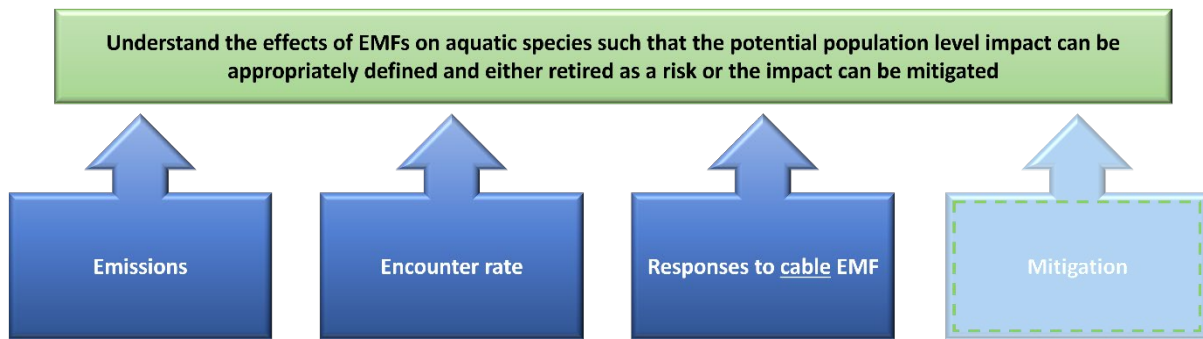


Figure 28. The evidence needs for an effective approach to predicting EMF impacts on focal receptors in the aquatic environment. The likelihood of encounter assessment can be considered a precursor to build upon in establishing an encounter rate for a species that is likely to encounter an EMF.

7. Discussion and Recommendations

WP2 has proposed an approach that enables an effective assessment of the likelihood of encounter between focal receptors and EMFs associated with offshore wind developments. Further, a structured framework is provided with guidance through demonstrating the application to dynamic cabling through a floating offshore wind case study. It is recognised that this represents an initial early stage in the assessment of the likelihood of encounter. However, the proposed stepwise framework approach should address some of the uncertainty surrounding EMFs and their potential significance to receptive species in the marine environment. Whilst it is acknowledged that the topic of receptor species responses to EMFs associated with subsea power cables is poorly understood (Hutchison et al., 2020a, 2021; Taormina et al., 2018), determining the likelihood of encounter with the subsea power cable (SPC) EMFs is relatively straightforward and can help indicate whether EMFs need consideration early in the EIA scoping stage. This should speed up the initial decision-making process and inform whether EMFs should be included in an Environmental Impact Assessment.

In the following sections, the results of WP2 are discussed and the limitations of the evidence used within the framework identified with recommendations to advance the proposed methods.

7.1 Cable magnetic field measurements

There were some consistent findings from the fieldwork, regardless of the type of cable or location. For most sites where the cable axis was correctly identified, the highest magnetic field intensity was observed directly above the cable. The intensity decreased with distance from the cable, most notably near the cable. However, whilst the intensity of the field dropped rapidly over the first few metres, following a $1/r^2$ relationship, the dissipation occurred over a greater distance than predicted by the models. The magnetic field intensity remained within the expected detectable range of receptor species for several metres, in most cases for tens of metres.

Another factor that should be considered is the number of cables at a site, as most of the sites that we surveyed did not have a single export cable. The proximity of other cables increased the extent of the magnetic field generated by the subsea power cables, which consequently must be considered when assessing the likelihood of EMF encounter for receptors. At some sites, there were cables from other wind farms or interconnectors; and as multiple cables produced multiple sources of EMF emissions, all EMF sources at a site should be considered in terms of their cumulative effects and not simply in isolation. A cumulative assessment may well be more representative of what a receptor may be exposed to in the marine environment.

During the fieldwork we visited multiple sites, which strengthened the evidence base and the conclusions that we were able to draw from the real measurements of magnetic fields, in comparison to modelled outputs. Unfortunately, it was not possible to use all the measurement data in the comparison study owing to a lack of the necessary cable parameter data required for accurate modelling.

Some of the key data were provided by the wind farm and cable operators, which highlights the importance of engagement with the industry in accessing relevant input parameters. However, the data did not always include the information needed for the model parameterisation. In particular:

- The actual burial depth was not available; therefore, the best approximation was made using the 'as-built' data. Several sites are subject to regular changes in coastal substrate movement (either erosion or deposition), and therefore, the 'as-built' depths will not be sufficient in such cases.
- For Horizontal Directional Drilled (HDD) cables the depth was not always reported.
- Power output data are essential to determine the electrical current in the cable at the time of measurement; however, the form of the power data varied from sub-second reading to averaged data over set periods.
- The availability of the cable specifications also varied, particularly the relationship between the conducting cores and the twist (or helix/lay length), which was only reported in a few cases.

These limitations in the availability and reporting format of data highlight the need for consistent and comparable reporting processes, including improved parameter information and more readily available access.

7.2 Comparing measured and modelled magnetic fields

The comparison between modelled and measured magnetic field data for the specific current in the cable at the time of measurement revealed a discrepancy. This was apparent for each of the sites considered. The models predicted that the magnetic field intensity would decrease at approximately $1/r^2$, which was a more rapid decline than the measured data showed. The $1/r^2$ propagation is associated with the primary currents within each conductor and their interaction within an AC cable, which is termed the phase-current.

The basic models focus on the phase-current, and they assume the conductor cores are linear and parallel; therefore, the models neglect any twist in the cables. Most 3-core AC cables have a twist, which should be accounted for in understanding the resultant magnetic field generated. With increased twisting, there will be some cancellation of the magnetic fields produced during transmission of electrical current, which will alter the propagation distance of the magnetic field (Pettersson and Schonborg, 1997). If the twist of the cable is larger than the distance away from the cable axis where the magnetic field is modelled or measured, then the assumption of linear cores is appropriate. Therefore, the periodicity of the twists along the cable's length should be determined and taken into account in a model to be more representative of the real situation (as proposed by Gill et al. 2023). Data on the cable twist are therefore essential when modelling the EMFs of SPCs.

The propagation of the magnetic field did not follow the $1/r^2$ predicted relationship. Overall, it was nearer to $1/r$. Whilst phase-currents dominate close to the cable (within a few metres), during the transmission of electrical current along a conductor there are sheath currents. With three conductors, the sheath currents may be unbalanced. Therefore, the influence of one conductor could be greater if the magnetic field is modelled or measured further away from the cable. As a result, there is a net current present, which is predicted to influence the magnetic field at a distance where the phase current is much reduced. The net current will become dominant, which is predicted by a $1/r$ relationship (EPRI 2022). In the case of our measurements, as the cables were buried, we most likely captured part of the phase currents within the first few metres. However, most of our measurements are likely to be linked to the net currents. The transition where the net current takes over from the phase-currents appeared to be in the 5-10 m zone for the cables that we could compare. Therefore, measurements closer to the cable would be beneficial, particularly when assessing dynamic cables, which are not buried. The phase currents of dynamic cables will be expected to be dominant at the surface and within metres of the cable in the water column, with the net currents propagating greater distances.

To understand the likely EMF environment associated with a subsea cable (whether buried or not) at known distances from the cable, the assessment should apply the following:

$$\begin{array}{c|c|c|c} \text{Magnetic field (at a point in the environment)} & = & \text{Phase current magnetic field (at the same point)} & + \text{Net current magnetic field and phase current (at the same point)} \end{array}$$

The estimated values of the magnetic fields are most likely to be reported as RMS, particularly in models. Other units of measurement are sometimes used, namely Peak-Peak or zero-Peak; all three units are easy to convert between. It is, however, essential that the EMF units are clearly stated, whether magnetic or electric fields.

7.2.1 Variability in EMFs

During the approximately one-hour periods that we measured the magnetic fields, there were power fluctuations at some sites. This is not an unexpected occurrence with offshore wind technology. Furthermore, with the alternating nature of the electrical current being transmitted in the HVAC cables, the magnetic field reached different maxima and minima with increasing distance from the cable. The highest positive and negative peaks of the magnetic field intensity were often observed near the cable. From a receptor's perspective, this suggests that the EM-environment is more variable nearer to a cable and therefore less predictable. For the sake of realism, it is crucial to include magnetic field variability in the models, as presently they focus on the maximum power and assume that the EMF remains at that level or that is the worst-case scenario which may not be accurate. Evidently, this is too simplistic as it assumes that the maximum intensity is the main information required; it does not assist with the reality of assessing the extent, intensity and the variability of the EMFs, which is necessary when interpreting the emission with regards to the receptors of interest. From the perspective of the receptors, it is the variability in the sensory environment that is required to be understood, as they often respond to changes that occur over time. A receptor will better learn about their environment if stimuli are predictable and less variable (Hutchison et al 2021).

7.2.2 A note on electric fields

A final point worthy of note, regarding cable EMFs, is that of the comparison between models and measurements discussed here relates to the magnetic fields. The primary factor in the magnetic field being present is the electrical current being transmitted through the cable core(s). There are electric fields within the cable, but they are shielded by the cable materials. However, in an AC cable with more than one conductor, the rotation of the magnetic fields induces electric fields outside of the cable into the external environment. While the electric fields are challenging to measure, they will only occur in the water, so they cannot be measured in the air or on the beach above the cable. Modelling these induced electric fields is feasible as long as the appropriate parameters are available but is not routinely undertaken (see Appendix 1; Gill et al 2023).

7.3 Receptors

Current practice when assessing the impact of EMFs on receptors within the environmental assessment process is to model the magnetic field associated with a single cable and report the maximum intensity of the field. Clearly, as most sites do not have single cables (demonstrated in Section 3), then the relationship between the number of cables, the distance between them and the variability in power transmission should be considered in order to represent the EMF environment that the receptor may be exposed to.

It is also current practice to focus on the maximum EMF intensity and the drop-off distance of the propagating EMFs. The focus on maximum EMF intensity relies on the assumption that greater EMFs are worse for receptors than lower EMFs, and that the decline in intensity with distance from the cable is consistent with the EMF modelling predictions. It was evident during the field measurements that in most cases, the magnetic field values fell within the known detection range of receptors over specific distances from the cable (). Within these magnetic field ranges, behavioural, physiological and/or developmental responses may occur (Albert et al., 2020; Gill and Desender 2020; Hutchison and Gill, 2025). The potential impact of magnetic fields will be directly related to the amount of exposure of the receptor to the fields as well as the intensity (see Section 5.1). Therefore, the distance from the cable at which the intensity reduces to below the detectable range should be determined to effectively assess the spatial zone of potential encounter and subsequently, any potential impact (or to justify scoping EMF out of the EIA). The main caveat for this recommendation is that the range of detection is poorly understood for most species. Therefore, the confidence in determining any impact will likely be low. More research is needed to understand what constitutes a typical detection range for different receptive species, to improve confidence in the assessment.

7.3.1 Spatial outputs for species occurrence and distribution, and cable routes

The occurrence and distribution of the species were estimated using the proxy of habitat suitability in Section 4. The habitat suitability models used represented the best available data based on several years of offshore surveys, using standard international methods. However, these offshore datasets have poor coverage of near shore areas where sampling was not possible owing to gear and safety risks. Therefore, if there is overlap between species occurrence and EMF zones in the offshore environment and there are missing data for nearshore habitats (i.e. blank grid squares in the GIS outputs), then it is necessary to consider a targeted data search or collection of supplementary data, which may require a different sampling approach or equipment. An alternative may be to model or consider expert elicitation in the absence of data and timely approaches, until data collection may be undertaken. The absence of data in the nearshore, relate to both the spatial and temporal use of the shallower coastal waters. This is particularly important for the early life stages, as many species use nearshore habitats as a refuge for larvae and juveniles, or for migration routes, and it is in shallower coastal areas where EMFs are more likely to propagate up to the surface

(noting that the intensities and extent of the EMFs in these waters will be lower if cables are further away from the surface water due to being buried deeply or horizontally directionally drilled).

The maximum spatial extent of the magnetic field zone that we applied around the offshore wind developments and cable routes was selected based on the lowest known magnetic field intensity within the range that is known to elicit a response by a receptor. However, the data for that intensity are based on one or two species and are unlikely to be fully representative of receptor species in general; therefore, it is essential to note that the sensory ranges will be specific to the species of interest (and it should be determined whether it is the sensory range for magnetic fields, electric fields or both that is applicable to the focal receptor). In future, as evidence on species-specific response becomes available, the EMF zones can be adjusted, which in time will increase the confidence in these likelihood of encounter assessments.

7.4 The framework

The framework for the likelihood of encounter assessment was applied in a step-by-step manner to the floating offshore wind case study, with the focal receptor as the adult basking shark. Following the steps through the guidance in Section 6 illustrated clearly how to determine the likelihood of encounter between the receptor and the defined EMF zone in 2D, 3D and temporally, with a clear indication of the confidence in the data used in the assessment. As such, the framework can be applied generally and can be used as a useful guide to incorporate EMF effects into the EIA scoping stage to decide whether EMFs need to be scoped into the environmental impact assessment process. This guidance makes the best possible assessment of the likelihood of a receptor to encounter EMFs based on current knowledge within the scoping-stage of the EIA process but does not advise on subsequent steps, however where relevant, aspects are highlighted that could be useful later in the EIA process.

7.5 Evidence gaps

In this WP, while acknowledging the limited information relating to both the subsea power cable EMFs and species response, we developed an effective approach to assess the likelihood of encounter between species and SPC EMFs. The likelihood of encounter approach provides a way to better consider the potential for a receptor to experience exposure to SPC EMFs and can be used early in the consideration of environmental impacts of offshore wind SPCs (both fixed and floating) and other transmission SPCs. Below, we identify key evidence gaps and propose actions to address them, with the aim of significantly improving confidence in future assessments.

7.5.1 Subsea power cable EMFs

- Cable EMF spatial extent is determined by the intensity and propagation of magnetic fields induced by the transmission of electrical current through a subsea power cable. Offshore wind power generation varies according to the wind resource, therefore the magnetic field modelled should be able to reproduce this variability based on the power transmission data, where available.
- Basic data on the cables' properties and characteristics are required for modelling. This should include both phase currents and net currents for realistic model outputs.
- Accurate and accessible information on the location of the cables (e.g. as laid depth of burial for fixed offshore wind; depth of deployment for floating offshore wind) is a key requirement.

- The characteristics of the cable, including the twist, should be clearly determined to provide realistic estimations of the EMF extent and propagation properties.
- Electric fields can be estimated/modelled in the case of HVAC cables as they will be directly induced from the AC current. However, they will also require validation by comparing measured and modelled electric fields.
- For HVDC cables there should be EMF modelling which considers the water movement and the movement of the animals as they induce electric fields within the range of detectability of receptors (see Gill et al 2023).
- Within the environmental assessment scoping, the RMS estimated values of the magnetic fields are most likely to be reported, particularly if EMF modelling is used. Other units of measurement are sometimes used, namely Peak-Peak or zero-Peak, all three units are easy to convert between. It is essential that the EMF units are clearly stated, whether magnetic or electric fields. What the receptors respond to is currently debate and should be explored further for both magnetic and electric field components.
- Methodologies to measure the EMFs of dynamic cables close to the surface of the cable should be developed to better understand the EMF characteristics close to the cable core and thereby improve the modelling validation. Further, methodologies to understand the influence of the dynamic cable flex and movement in the water column should be progressed.

7.5.2 Receptors

- Finer-scale data on focal species' spatial occurrence and density would improve the likelihood of encounter assessment.
- More data on three-dimensional (3D) habitat use over time would help better estimate the spatial and temporal overlap between EMF and receptor species and can advance towards being a quantitative assessment.
- Each life stage should be considered in the likelihood of encounter assessment; however, it is acknowledged that early life stage data are often limited.
- Improved availability of species distribution data in nearshore waters is required, particularly as this is where animals are more likely to encounter EMF owing to the shallower water depths and the convergence of export cable routes to landfall. Although, if HDD is used then the extent and intensity of EMF at the seabed encountered will be towards the lower end of the range of detectability because of the greater distance between the cable and any receptors. Until species-specific detection abilities are refined, this cannot be confirmed.
- Including the bathymetry data along cable routes where EMFs will occur would enhance the consideration of overlap in the likelihood of encounter assessment. Cross-sectional data from cable 'target burial depths(which are submitted with planning applications) are therefore a key requirement. Once cables are in the water, assessments should be updated with 'as laid' cable data.
- Our focus in WP2 was the magnetic fields. We did not take into account the electric fields, which will also be present. Therefore, interpretation of the predicted fields is relevant for the magneto-sensitive species. However, the interpretation for electrosensitive species should be treated as an incomplete assessment of the likelihood of encounter of EMFs and subsequently treated with caution until electric field data or modelled estimates can be provided.

- The lack of knowledge on the actual sensitivity of a range of receptor species within the range of EMFs associated with subsea power cables is a real limitation for the interpretation of the outcome of an encounter with EMFs. To improve the confidence in the determination of potential environmental impact further studies are required to specifically address this knowledge gap.

8. Acknowledgements

Many thanks to Marieke Desender, a former Cefas colleague for her important contribution to the initial stages of this study, and particularly the field survey coordination. WP2 would not have been possible without the engagement of the offshore transmission operators and wind farm operators, who provided critical data for the field measurements and use in the modelling.

9. References

Andrzejaczek, S., Lucas, T.C.D., Goodman, M.C., Hussey, N.E., Armstrong, A.J., [...] Curnick, D.J. (2022). Diving into the vertical dimension of elasmobranch movement ecology. *Sci. Adv.* 8, eabo1754. DOI:10.1126/sciadv.abo1754 <https://www.science.org/doi/pdf/10.1126/sciadv.abo1754>.

Austin, R.A., Hawkes, L.A., Doherty, P.D., Henderson, S.M., Inger, R., Johnson, L., Pikesley, S.K., Solandt, J.-L., Speedie, C., Witt, M.J. (2019). Predicting habitat suitability for basking sharks (*Cetorhinus maximus*) in UK waters using ensemble ecological niche modelling. *Journal of Sea Research*, 153, 101767. <https://doi.org/10.1016/j.seares.2019.101767>.

Bresesti, P., Kling, W.L., Hendriks, R. L. & Vailati, R. (2007) HVDC Connection of Offshore Wind Farms to the Transmission System. *IEEE Trans. on Energy Conversion* 22 (1): 37 – 43.

Couce, E., Pinnegar, J.K., Townhill, B.L. (2025). Climate change resilience of vulnerable marine species in northwest Europe. *Mar Biol* 172, 116. <https://doi.org/10.1007/s00227-025-04672-x>.

Doherty, P.D., Baxter, J.M., Gell, F.R., Godley, B.J., Graham, R.T., Hall, G., Hall, J., Hawkes, L.A., Henderson, S.M., Johnson, L., Speedie, C., Witt, M.J. (2017). Long-term satellite tracking reveals variable seasonal migration strategies of basking sharks in the north-east Atlantic. *Sci Rep.*, 7:42837. doi: 10.1038/srep42837.

Doherty, P.D., Baxter, J.M., Godley, B.J., Graham, R.T., Hall, G., Hall, J., Hawkes, L.A., Henderson, S.M., Johnson, L., Speedie, C., Witt, m.J. (2019). Seasonal changes in basking shark vertical space use in the north-east Atlantic. *Mar Biol* 166, 129. <https://doi.org/10.1007/s00227-019-3565-6>.

EPRI (2022). *Electric and Magnetic Field Management Reference Book: Second Edition*. EPRI, Palo Alto, CA: 2022. 3002024734.

England, S.J., Robert, D. (2022), The ecology of electricity and electroreception. *Biol Rev*, 97: 383-413. <https://doi.org/10.1111/brv.12804>.

GBIF (2021) Global Biodiversity Information Facility. Available online from <https://www.gbif.org/>.

Gill, A.B., Hutchison, Z.L., Desender, M. (2023). Electromagnetic Fields (EMFs) from subsea power cables in the natural marine environment. Cefas Project Report for Crown Estate Offshore Wind Evidence and Change Programme, 66 pp.

Hermans, A., Winter, H. V., Gill, A. B., & Murk, A. J. (2024). Do electromagnetic fields from subsea power cables effect benthic elasmobranch behaviour? A risk-based approach for the Dutch Continental Shelf. *Environmental Pollution*, 346, 123570.

Hunter E., Buckley A.A., Stewart C., Metcalfe J.D. (2005). repeated seasonal migration by a thornback ray in the southern north sea. *Journal of the Marine Biological Association of the United Kingdom*; 85(5): 1199-1200. Doi:10.1017/S0025315405012300. <https://doi.org/10.1017/S0025315405012300>.

Hutchison, Z.L., Gill, A.B., Sigray, P., He, H. and King, J.W. (2020a). Anthropogenic electromagnetic fields (EMF) influence the behaviour of bottom-dwelling marine species. *Scientific Reports*, 10(1), 1-15.

Hutchison, Z.L., Secor, D.H., Gill, A.B. (2020b). The interaction between resource species and electromagnetic fields associated with electricity production by offshore wind farms. *Oceanography*, 33(4), 96-107.

Hutchison, Z.L., Gill, A.B., Sigray, P., He, H., King, J.W. (2021). A modelling evaluation of electromagnetic fields emitted by buried subsea power cables and encountered by marine animals: Considerations for marine renewable energy development. *Renewable Energy*, 177, 72-81.

Korneliussen, R. J., Heggelund, Y., Macaulay, G. J., Patel, D., Johnsen, E., & Eliassen, I. K. (2016). Acoustic identification of marine species using a feature library. *Methods in Oceanography*, 17, 187-205. MMO (2014). Review of post-consent offshore wind farm monitoring data associated with licence conditions. A report produced for the Marine Management Organisation, pp 194. MMO Project No: 1031. ISBN: 978-1-909452-24-4. <https://www.gov.uk/government/publications/review-of-environmental-data-mmo-1031>.

Moriarty, M., Greenstreet, S.P.R., Rasmussen, J. (2017). Derivation of Groundfish Survey Monitoring and Assessment Data Product for the Northeast Atlantic Area. *Scottish Marine and Freshwater Science* Vol 8 no 16, 240pp. DOI: 10.7489/1984-1.

Newton, M., Barry, J., Lothian, A., Main, R., Honkanen, H., Mckelvey, S., Thompson, P., Davies, I., Brockie, N., Stephen, A., O'Hara Murray, R., Gardiner, R., Campbell, L., Stainer, P., Adams, C. (2021). Counterintuitive active directional swimming behaviour by Atlantic salmon during seaward migration in the coastal zone, ICES Journal of Marine Science, Volume 78, Issue 5, Pages 1730–1743, <https://doi.org/10.1093/icesjms/fsab024>.

Normandeau, Exponent, Tricas, T., Gill, A. (2011). Effects of EMFs from Undersea Power Cables on Elasmobranchs and Other Marine Species. U.S. Dept. of the Interior, Bureau of Ocean Energy Management, Regulation, and Enforcement, Pacific OCS Region, Camarillo, CA. OCS Study BOEMRE 2011-09. <https://www.boem.gov/sites/default/files/environmental-stewardship/Environmental-Studies/Pacific-Region/Studies/2011-09-EMF-Effects.pdf>.

Nyqvist, D., Durif, C., Johnsen, M.G., De Jong, K., Forland, T.N., Sivle, L.D. (2020). Electric and magnetic senses in marine animals, and potential behavioral effects of electromagnetic surveys. *Marine Environmental Research*, 155, 104888.

Pettersson, P. and Schonborg, N. (1997). Reduction of power system magnetic field by configuration twist. *IEEE Trans. Power Deliv.*, vol. 12, no. 4, pp. 1678-1683, DOI: 10.1109/61.634190

Resner, L., Paszkiewicz, S. (2021). Radial Water Barrier in Submarine Cables, Current Solutions and Innovative Development Directions. *Energies*, 14, 2761. <https://doi.org/10.3390/en14102761>.

Taormina, B., Bald, J., Want, A., Thouzeau, G., Lejart, M., Desroy, N., Carlier, A. (2018). A review of potential impacts of submarine power cables on the marine environment: Knowledge gaps, recommendations and future

directions, Renewable and Sustainable Energy Reviews, 96, 380-391.

<https://doi.org/10.1016/j.rser.2018.07.026>.

Townhill, B.L., Couce, E., Tinker, J., Kay, S., Pinnegar, J.K. (2023). Climate change projections of commercial fish distribution and suitable habitat around northwestern Europe. Fish and Fisheries, 24, 848-62.

<https://doi.org/10.1111/faf.12773>.

Wright, S., Griffiths, C.A., Bendall, V., Righton, D., Hyder, K., Hunter, E. (2024). Seasonal migrations of the European sea bass (*Dicentrarchus labrax* L.) in UK and surrounding waters. Mov Ecol 12, 45.

<https://doi.org/10.1186/s40462-024-00482-w>.

10. Appendices

1. **Appendix 1.** Parameters for modelling EMFs from Subsea Power Cables

Appendix 1. Parameters for modelling EMFs from Subsea Power Cables (Source Gill et al. 2023).

Cable parameters applicable for modelling EMFs for the purposes of permitting and research. Parameters are colour coded according to the applicability to modelling; energy emission only (orange, 1-3), energy emission in the marine environment (blue, 1-5), energy emission as it interacts with marine environment (green, 1-9), and the energy emission as it interacts with the marine environment with consideration of the motionally induced electric field (purple, 1-12), with an additional set of parameters to enhance the accuracy of the basic AC model (purple, 13-18). Applicability to the current type (DC/AC) and type of modelling (permitting (P) and/or research (R)), is indicated. Status reflects whether the parameter is typically included in modelling, ready to be incorporated in a model or if further exploration would be required to incorporate the parameter in an EMF model.

		Parameter	Unit	Description	DC/AC	Model Type	Status		
(a) Basic Cable EMF (emission only; assumes infinite length of conductor)									
1	1	1	1	Current	amps	The electrical current carried in the cable at a particular point in time.	DC/AC	P / R	Typical
2	2	2	2	Conductor Axes	x, y in metres	Relative coordinates of the centre of cable conductors so that it can be represented in the model domain. It will include the distance from the conductor core to the outer sheath.	DC/AC	P / R	Typical
3	3	3	3	Cable diameter	metres	Full diameter of the cable as per the technical specification.	DC/AC	P / R	Typical
(b) Cable EMF in Marine Environment									
4	4	4	4	Spatial position	qualitative	Spatial position in the marine/coastal environment: buried in the seabed, surface laid or in the water column. This would be reflected in the cable domain relative to the seabed/water surface, to aid interpretation of the model output.	DC/AC	P / R	Ready
5	5	5	5	Burial depth (if needed)	metres	Depth of burial is the distance from the outer surface of the cable to the seabed surface. 'Target burial depth' is data available prior to cable deployment. 'As laid burial depth' is preferable data once the cable is laid.	DC/AC	P / R	Ready/ To be explored
(c) Research additions (magnetic field)									
6	6	6	6	Geographic location	coordinates	The geographic location is an essential factor in determining the local geomagnetic field. The route of the cable and variation in terms of geography should be considered rather than a single point on the cable.	DC/AC	R	Ready – DC To be explored - AC
7	7	7	7	Altitude	metres	Vertical distance relative to mean sea level for a specific time and date will allow the geomagnetic field to be determined (x, y, z) for the above geographic location.	DC/AC	R	Ready – DC To be explored - AC
8	8	8	8	Orientation	degrees	Orientation of the cable relative to the geomagnetic field determines how the cable's magnetic field and geomagnetic field interact.	DC/AC	R	Ready – DC To be explored - AC
9	9	9	9	Protection permeability	henries/metre	If cable protections are used, the determination of the magnetic permeability would need to be included, if applicable.	DC/AC	R	Ready – DC To be explored - AC
(d) Research additions (motionally induced electric field)									

10	Boundary layer	reynolds number (dimensionless), velocity (m/s)	The water velocity in the boundary layer may be an influential factor in determining the motionally induced electric fields in near seabed scenarios, as well as exposed cable scenarios due to flow around the cable surface. Regional scale hydrodynamic models do not typically output boundary-layer flow velocities, however, a logarithmic boundary-layer model can estimate this from the near bed velocity from a 3D model.	DC/AC	R	To be explored
11	Sediment conductivity	siemens/m	Sediment porosity will influence the volume of water in the sediment and its movement through the sediment; therefore, it may affect the conductivity and the resulting propagation of the motionally induced electric field.	DC/AC	R	To be explored
12	Water conductivity & velocity	siemens/m, metres/sec	Water velocity and water conductivity (salinity) will determine the motionally induced electric field arising from the emitted magnetic field.	DC/AC	R	To be explored
(e) Research additions to improve AC modelling (to improve the accuracy of the basic cable EMF emission only model)						
13	Cable laylength	metres	The periodicity of the helical twist of the cable, recorded in metres.	AC	R	Ready
14	Sheath current	amps, root mean squared	The sheath current would be determined from the sheath's dimensions, plus the material and/or impedance and the bonding arrangement. [Note: current is not usually measured]	AC	R	Ready
15	Armour (if magnetic)	metres, henries/m	If the armour of the cable is magnetic, the dimensions of the armour (m) and the permeability of the material type should be included to provide an estimation of the armour screening effect from literature.	AC	R	Ready
16	Radius of conductors	metres	The radius of the conductors within the cable's core (in addition to the core coordinates).	AC	R	Ready
17	Harmonics	hertz, amps	The frequency at which the current is oscillating and multiples of that frequency. [The potential influence of the frequency may depend on the marine species sensitivity]	AC	R	Ready, To be explored
18	Cable length	metres	The specific position of the model scenario on the cable and the total length of the cable (most applicable to the cable in the marine environment).	AC	R	Ready